


2015

Synthesis and Evaluation of Substituted Coumarin Derivatives as Inhibitors of Monoamine Oxidase B

Ian A. Kieffer

Roger Williams University, ikieffer674@g.rwu.edu

Follow this and additional works at: http://docs.rwu.edu/chemistry_theses

 Part of the [Chemicals and Drugs Commons](#), [Diseases Commons](#), and the [Life Sciences Commons](#)

Recommended Citation

Kieffer, Ian A., "Synthesis and Evaluation of Substituted Coumarin Derivatives as Inhibitors of Monoamine Oxidase B" (2015).
Chemistry Theses. Paper 1.
http://docs.rwu.edu/chemistry_theses/1

This Thesis is brought to you for free and open access by the Feinstein College of Arts and Sciences Theses at DOCS@RWU. It has been accepted for inclusion in Chemistry Theses by an authorized administrator of DOCS@RWU. For more information, please contact mwu@rwu.edu.

**Synthesis and Evaluation of Substituted Coumarin Derivatives as
Inhibitors of Monoamine Oxidase B**

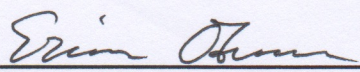
Ian A. Kieffer

Bachelor of Science in Chemistry
Department of Chemistry and Physics

Feinstein College of Arts and Sciences
Roger Williams University

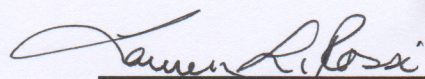
May 2015

The thesis of Ian A. Kieffer was reviewed and approved by the following:



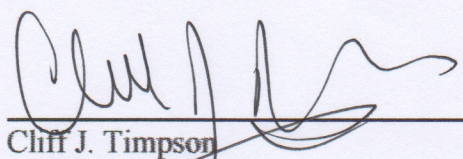
Erica L. Oduaran
Assistant Professor of Chemistry
Thesis Advisor

Date 4/17/2015



Lauren L. Rossi
Assistant Professor of Chemistry
Committee Member

Date 4/17/2015



Cliff J. Timpson
Professor of Chemistry
Committee Member

Date 17 APRIL 2015

Acknowledgements

I would like to thank Dr. Oduaran for her continued guidance and support throughout my time spent conducting research. I would also like to thank my thesis committee members Dr. Rossi and Dr. Timpson for the suggestions that they contributed to this work. Dr. Taylor is to thank for providing structure to the process of thesis writing. For funding for research supplies I would like to thank Marine & Natural Sciences senior thesis and the Roger Williams Foundation to Promote Scholarship and Teaching. I would also like to extend a thank you to the RWU Office of the Provost and Student Senate for providing funds to travel and present the research enclosed within this thesis at various national conferences. Lastly, I would like to thank the RI-INBRE Centralized Research Core Facility for assistance in acquiring mass spectra for the inhibitors prepared in this work, as well as the developers of UCSF Chimera for providing a means to perform computational docking studies of the inhibitors.

Table of Contents

Signature Page	ii
Acknowledgements.....	iii
Table of Contents.....	iv
List of Figures.....	v
Abstract.....	vii
1. Introduction.....	1
1.1 Monoamine Oxidase B as a Drug Target.....	1
1.2 Structural Analysis of Monoamine Oxidase B	3
1.3 The Need for MAO B Inhibitor Selectivity and Reversibility.....	5
1.4 Inhibitor Scaffold Selection & Diversification.....	7
1.5 Coumarin Inhibitor Preparation	9
1.5.1 Preparation of 7-benzyloxy Substituted Coumarins	9
1.5.2 Preparation of 3-aryl Substituted Coumarins.....	10
1.6 Experimentally Determining Inhibitor Potency and Reversibility	11
1.7 Docking Analysis to Probe the Enzyme Active Site	13
2. Experimental.....	15
2.1 Synthesis	15
2.1.1 Synthesis of 7-nitrobenzyloxy Substituted Coumarin Derivatives.....	15
2.1.2 Synthesis of 7-aminobenzyloxy Substituted Coumarin Derivatives	19
2.1.3 Synthesis of 3-(3-nitrophenyl)-6-methylcoumarin	20
2.2 Enzyme Inhibition Kinetics	21
2.3 Inhibitor Docking Experiments.....	22
3. Results.....	24
4. Discussion.....	31
4.1 Synthesis	31
4.2 Kinetics and Docking Scores.....	31
4.3 More Potent Inhibitor Structure Predictions.....	36
5. References.....	40
Appendix A. Attempted Synthetic Methodology	44
A.1 Preparation of 7-(4-aminobenzyl)oxy Substituted Coumarins	44
A1.2 Preparation of 3-nitrophenyl Substituted Coumarins.....	54
Appendix B. Synthesis Characterization Spectra	56

List of Figures

Figure 1	Common monoamine oxidase substrates.	2
Figure 2	Complex of 1,4-diphenyl-2-butene with a monomeric unit of human MAO B.	4
Figure 3	Structures of Clorgyline, an irreversible inhibitor of MAO A, and Pargyline, an irreversible inhibitor of MAO B.	6
Figure 4	Coumarin scaffold and substitution patterns for study.	8
Figure 5	Lineweaver-Burk plots for (A) competitive, (B) noncompetitive, and (C) uncompetitive inhibition. A blue line corresponds to no inhibitor being present and a red line corresponds to the presence of inhibitor.	12
Table 1	Results of inhibition kinetics for nine prepared compounds with respective docking scores.	24
Figure 6	Correlation between the inhibition constant, K_i , for 7-nitrobenzyloxy substituted coumarins and their respective docking scores.	25
Figure 7	Lineweaver-Burk plot of one concentration of 7-(2-nitrobenzyl)oxy-4-methylcoumarin inhibiting MAO B.	25
Figure 8	Lineweaver-Burk plot of two different concentrations of 7-(2-nitrobenzyl)oxy-3,4-dimethylcoumarin inhibiting MAO B.	26
Figure 9	Lineweaver-Burk plot of two different concentrations of 7-(3-nitrobenzyl)oxy-4-methylcoumarin inhibiting MAO B.	26
Figure 10	Lineweaver-Burk plot of two different concentrations of 7-(3-nitrobenzyl)oxy-3,4-dimethylcoumarin inhibiting MAO B.	27
Figure 11	Lineweaver-Burk plot of three different concentrations of 7-(4-nitrobenzyl)oxy-4-methylcoumarin inhibiting MAO B.	27
Figure 12	Lineweaver-Burk plot of two different concentrations of 7-(4-nitrobenzyl)oxy-3,4-dimethylcoumarin inhibiting MAO B.	28
Figure 13	Lineweaver-Burk plot of three different concentrations of 7-(3-aminobenzyl)oxy-4-methylcoumarin inhibiting MAO B.	28

Figure 14	Lineweaver-Burk plot of two different concentrations of 7-(3-aminobenzyl)oxy-3,4-dimethylcoumarin inhibiting MAO B.	29
Figure 15	Lineweaver-Burk plot of three different concentrations of 3-(3-nitroaryl)-6-methylcoumarin inhibiting MAO B.	29
Figure 16	MAO B activity plot at substrate concentration of 2.5 mM over 20 minutes.	30
Figure 17	Beer's law plot for resorufin at 571 nm.	30
Figure 18	Docking score calculated for 3-(3-aminophenyl)-6-methylcoumarin.	33
Figure 19	Docking of 3-(3-aminophenyl)-6-methylcoumarin to MAO B.	34
Figure 20	Docking of 7-(3-nitrobenzyl)oxy-4-methylcoumarin to MAO B.	35
Figure 21	Docking of 7-(3-aminobenzyl)oxy-4-methylcoumarin to MAO B.	35
Figure 22	Docking of 3-(3-nitrophenyl)-6-methylcoumarin to MAO B.	36
Figure 23	Docking of 3-(3-aminophenyl)-6-hydroxycoumarin to MAO B.	37
Figure 24	Docking scores of several coumarins with structures analogous to 3-(3-aminophenyl)-6-hydroxycoumarin were found to be more potent computationally than 3-(3-aminophenyl)-6-methylcoumarin.	38

Abstract

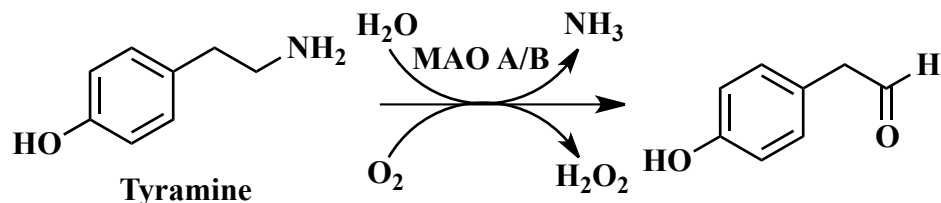
Monoamine oxidase B (MAO B) is of clinical importance due to its perceived role in neurodegenerative diseases such as Parkinson's, making inhibitors of MAO B popular candidates for drug design. A series of coumarin derivatives have been prepared and assayed, revealing that the synthesized inhibitors act through a competitive mode of inhibition. In addition, these inhibitors are potent with K_i values in the nanomolar range. Overall, substitution at the 3- position of the coumarin was found to be important to inhibitor potency and further study of 3-aryl coumarin substitution computationally led to the prediction of 3-(3-aminophenyl)-6-hydroxycoumarin as a lead compound for future study as a more potent MAO B inhibitor.

1. Introduction

1.1 Monoamine Oxidase B as a Drug Target

Monoamine oxidases are enzymes of the outer mitochondrial membrane that catalyze the oxidative deamination of neurotransmitters and dietary amines, as shown in Scheme 1.¹

Scheme 1.



Because of the importance of these enzymes in the metabolism of key neurotransmitters monoamine oxidases are of great clinical importance for treatment of both neurological and psychiatric diseases. Two isoforms of differing substrate selectivity exist for monoamine oxidase: the A form (MAO A) and the B form (MAO B). While MAO A preferentially deaminates the neurotransmitters serotonin, epinephrine, and norepinephrine, MAO B preferentially deaminates benzylamine and phenethylamine, as shown in Figure 1.² Dopamine, tyramine, and tryptamine are substrates for both MAO A and MAO B.

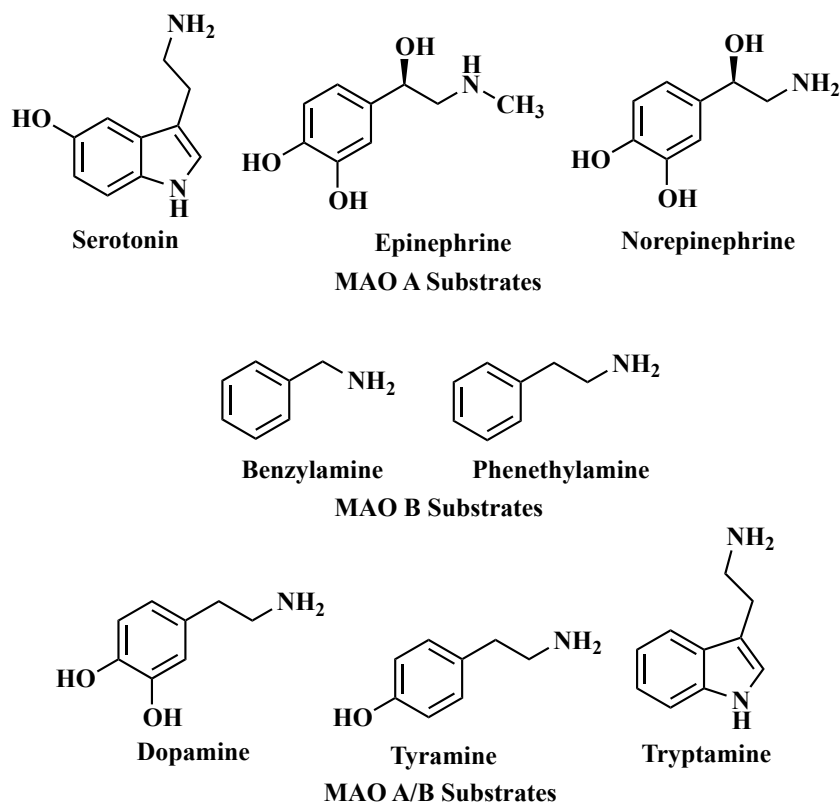


Figure 1. Common monoamine oxidase substrates.

The substrate specificities determine each isoform's respective clinical importance. Inhibition of human MAO A is associated with clinical effects relating to anti-anxiety and anti-depression.³ MAO A inhibitors are currently being used to treat depression and anxiety.⁴ Human MAO B, on the other hand, has been shown to get upregulated with age, being expressed four times as much at old age. More hydrogen peroxide, a reactive oxygen species known to further react and cause oxidative stress, is produced in this case.⁵ This oxidative stress is a likely cause of neurodegenerative diseases such as Alzheimer's and Parkinson's disease.^{3,5} Both MAO A and MAO B contain FAD binding domains with FAD covalently bound to a cysteine residue within each enzyme.⁶ This FAD cofactor functions to receive two electrons and two protons in the oxidative deamination reaction to form FADH₂. In order for the enzyme to perform another

catalytic turnover these hydride ions, H^- , are displaced onto O_2 , yielding H_2O_2 . Inhibition of MAO B can counteract the increased rate of hydrogen peroxide production that results from age, thus providing protection from oxidative stress, in turn, allowing for treatment or prevention of these and other neurodegenerative diseases. Currently, MAO B inhibitors are already being used to treat Parkinson's disease.⁷

1.2 Structural Analysis of Monoamine Oxidase B

MAO A is composed of 527 amino acids, while MAO B is made up of 520 amino acids.⁸ Overall, 70% of the amino acid identity of the isoforms is shared.⁸ The structures of both MAO A and MAO B have been elucidated by x-ray crystallography.⁹ MAO A crystalizes as a monomer, while MAO B crystalizes as a dimer.^{10,11} Furthermore, their respective active sites have been crystalized with inhibitors bound in order to provide information about the active site. The chain-fold of human MAO A is similar to that of human MAO B with MAO A possessing an active site that is a hydrophobic cavity of volume of nearly 550 \AA^3 .¹⁰ On the other hand, MAO B consists of a 420 \AA^3 hydrophobic substrate cavity attached to an entrance cavity of 290 \AA^3 , as shown in Figure 2.¹²

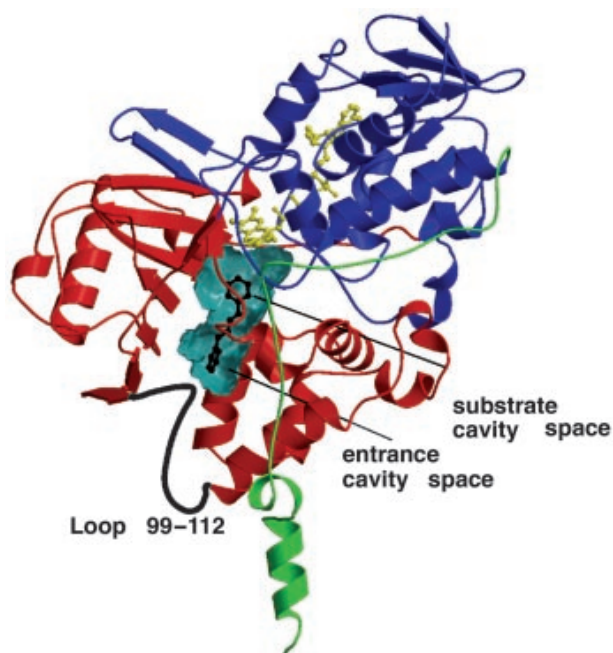


Figure 2. Complex of 1,4-diphenyl-2-butene with a monomeric unit of human MAO B. Within the three-dimensional structure, the FAD-binding domain (residues 4-79, 211-285, and 391-453) is blue, the substrate-binding domain (residues 80-210, 286-390, and 454-488) is red, and the C-terminal membrane-binding region is green. The FAD cofactor and the inhibitor are shown as yellow and black ball-and-stick models, respectively. The inhibitor binds in a cavity (the cyan surface) that results from the combination of the entrance and substrate cavities. Adapted from reference 13.

The MAO B binding site appears longer and flatter than the binding site of MAO A.¹⁴ Within MAO B the recognition site for the amino group of the substrate is an aromatic cage formed by Tyr 398 and Tyr 435.¹² Tyr 326 of MAO B is believed to play a critical role in determining the substrate and inhibitor specificities of the active site.¹⁵ This residue is located in the entrance cavity while Tyr 398 and Tyr 435 are located deeper within the enzyme and are part of the active site cavity. The cavity of the active site of MAO B is largely apolar with hydrophilic regions existing near the flavin.¹³ These regions help to direct the substrate for binding and catalysis.¹³ The loop consisting of residues 99-112 is responsible for allowing substrates into the entrance cavity so that they

may proceed to the active site.⁹ In addition, it appears Ile 199 in this isoform acts as a gate between the entrance cavity and the substrate cavity with rotation of this side chain allowing for the separation and fusion of the two cavities.¹³ This functionality is required to allow the substrate or inhibitor into the cavity of the active site. An understanding of the active site of MAO B can give insight as to why certain molecules are good substrates or inhibitors.

1.3 The Need for MAO B Inhibitor Selectivity and Reversibility

In the pursuit of inhibitors of MAO B it is important to realize several attributes an inhibitor of MAO B must possess in order to be considered a possible structure for clinical inhibition of MAO B. First, an inhibitor must be selective in its enzyme target. Without selectivity, a single compound may inhibit both MAO A and MAO B. This sort of interaction between the inhibitor and multiple enzymes leads to side effects when the inhibitor is taken as a drug. For this reason it is desirable for an inhibitor to be selective. Selectivity can be measured as the difference between pIC₅₀ values for inhibition of isoforms with the same inhibitor and should be $\geq \sim 3$, where the pIC₅₀ is $-\log(\text{IC}_{50})$.¹⁶ The IC₅₀ is the concentration of inhibitor that causes 50 percent inhibition of an enzyme catalyzed reaction. This definition of selectivity will be used in selecting attributes for inhibitor design later in the thesis. It is important to note that an inhibitor can be active for both isoforms, but the selectivity can greatly favor activity for one enzyme over another. Inhibitor selectivity studies were not performed in this work.

Binding between the inhibitor and the enzyme can be either reversible or irreversible. Irreversible inhibition often involves the formation of a covalent bond

between the inhibitor and the enzyme, whereas reversible inhibition is usually the result of intermolecular forces stabilizing the interaction between the inhibitor and the enzyme's active site. Clorgyline is an irreversible inhibitor of MAO A, while pargyline is an irreversible inhibitor of MAO B.^{17,18} Both of these inhibitors are strongly selective towards one isoform and their respective structures can be found in Figure 3.

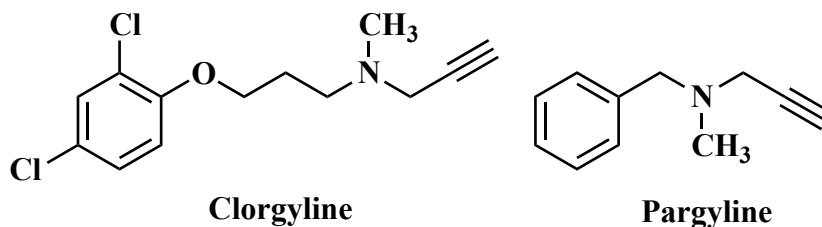


Figure 3. Structures of Clorgyline, an irreversible inhibitor of MAO A, and Pargyline, an irreversible inhibitor of MAO B.

Although these inhibitors are effective for inhibition of their corresponding amine oxidase targets, the ability of inhibitors to bind reversibly is of clinical importance. This is because several medical crises can result from the inhibitor not dissociating from the enzyme. Monoamine oxidases are required for the biological function of humans and an inhibitor binding to them irreversibly creates a problem in that they can no longer catalyze their needed reactions. Hypertensive crisis, for example, is one effect that can result from MAO inhibitors not dissociating.⁹ For this reason inhibitors of MAO B should be reversible if they are intended to be used clinically. Three types of reversible inhibition exist. In competitive inhibition the inhibitor binds to the enzyme active site, in noncompetitive inhibition the inhibitor binds to a site on the enzyme that is not the active site (these inhibitors do not impact substrate binding), and in uncompetitive inhibition the

inhibitor binds to the enzyme substrate complex at a site on the enzyme other than the active site.

1.4 Inhibitor Scaffold Selection & Diversification

A variety of molecular scaffolds have been shown to be useful for selective, reversible inhibition of MAO B. Coumarin derivatives of both synthetic and natural origin have been shown to be generally selective, reversible inhibitors of monoamine oxidase.⁹ In addition, crystallographic structures of MAO B co-crystalized with inhibitors have been obtained, increasing the depth of knowledge with regards to how inhibitors interact with the active site.⁹ Coumarin derivatives, in particular, have been co-crystalized with MAO B, highlighting their competitive mode of inhibition.¹⁹ Most of the potent and selective MAO B coumarin inhibitors thus far have been too lipophilic and had poor solubility in aqueous solutions, factors which limit their clinical exploration.²⁰ Therefore, further exploration of the coumarin scaffold is warranted. Although many substitution patterns of coumarin have been shown to be useful for reversible, selective inhibition of MAO B, derivatives containing 7-benzyloxy and 3-aryl substitution were the focus of this work and are shown in Figure 4.

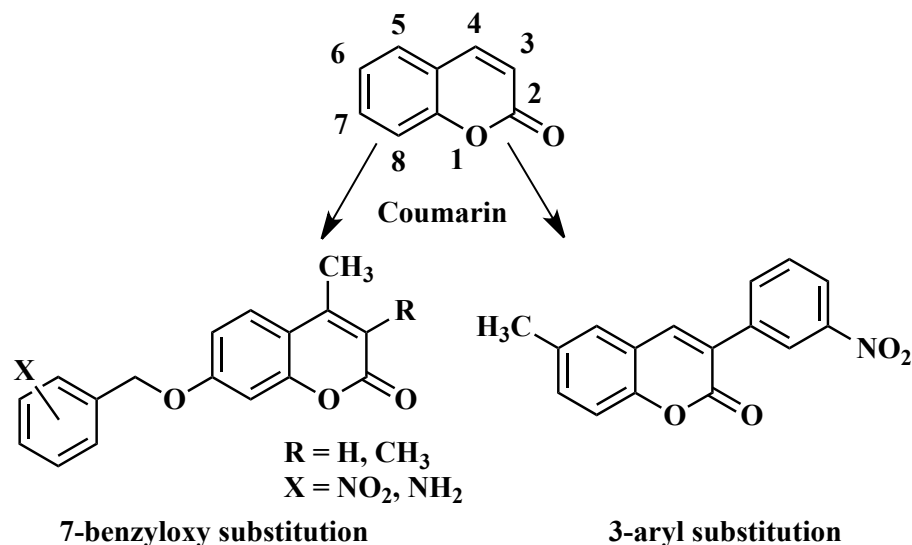


Figure 4. Coumarin scaffold and substitution patterns for study.

Coumarin derivatives possessing 7-benzyloxy substitution have proven to be effective inhibitors of MAO B, possessing good binding affinity (nanomolar concentrations of inhibitor needed for IC₅₀) and selectivity.^{16,21} Furthermore, these derivatives have been shown to be reversible inhibitors of MAO B. Methyl substitution at the 3-position of the coumarin scaffold in the presence of 7-benzyloxy substitution has been shown to increase the inhibitor's selectivity towards MAO B.¹⁶ When both the 3-methyl and 4-methyl substitution were not present the molecule's ability to inhibit was reduced.¹⁶

3-aryl substitution of coumarin has also been shown to result in selective, reversible inhibitors of MAO B.²² The addition of 6-methyl substitution on the coumarin was found to aid in both selectivity and potency.²² Larger substituents at the 6-position of the coumarin, however, are not as favorable due to steric interferences between the

inhibitor and the active site of MAO B.²² In addition, nearly all *ortho*-substitution of the 3-aryl ring has been found to be unfavorable.²²

Herein nitro and amino derivatives of 7-benzyloxy and 3-aryl substituted coumarins are prepared as they have not been fully explored in the literature yet as inhibitors of MAO B. This then suggests that further diversification of these scaffolds could result in more potent coumarin-based MAO B inhibitors than are currently known.

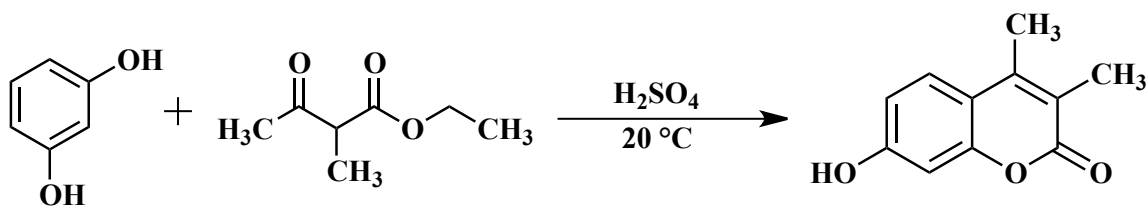
1.5 Coumarin Inhibitor Preparation

1.5.1 Preparation of 7-benzyloxy Substituted Coumarins

Preparation of 7-nitrobenzyloxy Substituted Coumarins

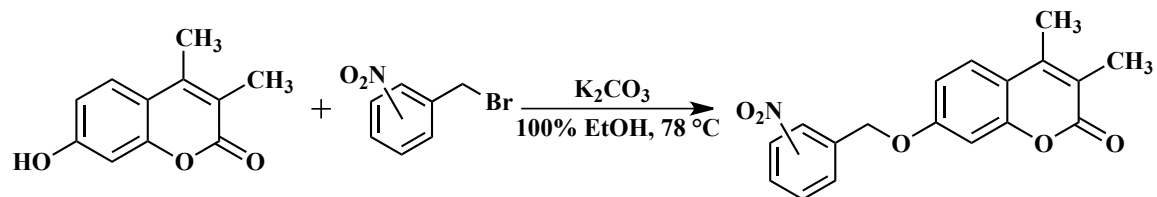
The desired 7-nitrobenzyloxy substituted coumarins can be prepared by reaction of the appropriate 7-hydroxy substituted coumarin with the appropriately substituted nitrobenzyl bromide. The Pechmann condensation of phenols with β -keto esters in the presence of a protic or Lewis acid is one way to generate 7-hydroxy substituted coumarins, as shown in Scheme 2.^{23,24}

Scheme 2.



The Williamson ether synthesis can be used to form the 7-nitrobenzyloxy substituted coumarin derivatives through coupling of the 7-hydroxy coumarin with the appropriately substituted benzyl bromide, as shown in Scheme 3.²⁵

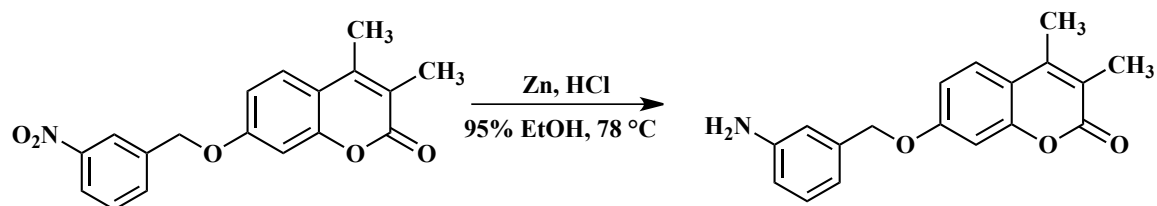
Scheme 3.



Preparation of 7-aminobenzloxy Substituted Coumarins

To prepare 7-aminobenzloxy substituted coumarins a reduction of previously prepared 7-nitrobenzloxy substituted coumarins can be performed. This reduction is mediated by zinc and uses hydrochloric acid as a hydrogen source and is shown in Scheme 4.¹⁶

Scheme 4.

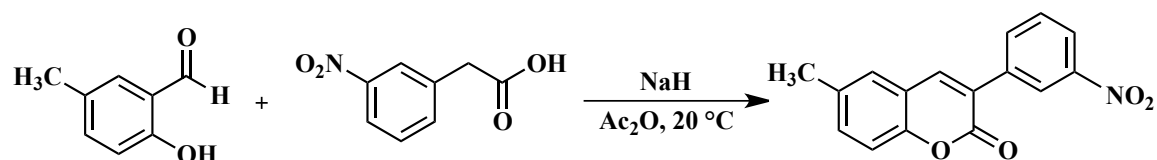


1.5.2 Preparation of 3-aryl Substituted Coumarins

Preparation of 3-nitroaryl Substituted Coumarins

To prepare the 3-nitroaryl substituted coumarin derivatives a modified Perkin reaction, Scheme 5, can be utilized.^{22,26,27}

Scheme 5.



1.6 Experimentally Determining Inhibitor Potency and Reversibility

To determine the potency of the synthesized inhibitors enzyme kinetic assays were performed with differing substrate concentrations (S) in the presence of the inhibitor (I). The catalytic conversion of the substrate to the product by the enzyme was measured by assessing the amount of product present in a sample at a given point in time. Several inhibitor concentrations are tested, along with control which contained no inhibitor, in order to generate plots of the product's concentration versus time. The slope of this line, the reaction's velocity (V), with respect to the various substrate concentrations was used to generate a Lineweaver-Burk plot ($1/V$ versus $1/[S]$) for each prepared inhibitor. The x-intercept of the best-fit line of this plot is equal to the K_m , the Michaelis-Menten constant. This same point in the presence of inhibitor is equivalent to the apparent K_m ($K_{m, app.}$). The Michaelis-Menten constant is the concentration of substrate at which the velocity is half of its maximum. Knowing these values allows for the calculation of the inhibition constant, K_i , by Equation 1.

$$K_i = \frac{K_m[I]}{K_{m, app.} - K_m} \quad (1)$$

The potency of synthesized inhibitors can be determined and compared quantitatively using the K_i value. As this value gets smaller, the potency of the inhibitor is greater – less inhibitor is required to achieve the same level of inhibition as a less potent inhibitor (higher K_i). An inhibitor is deemed potent for the purposes of this work if its IC_{50} or K_i is in the nanomolar (nM) range ($pIC_{50} = 9.0$). The K_i value is preferred herein because the IC_{50} is dependent on the substrate concentration used in the assay, making it difficult to make direction comparison to literature values without specific details of their assays.²⁸

The K_i value is also preferable because its determination provides insight into the mode of inhibition.

Analysis of the Lineweaver-Burk plot and the y-intercepts of its various inhibitor concentration curves allows for determination of the inhibitor's mode of inhibition. If the y-intercept (maximum velocity) of the substrate with no inhibitor is the same as the substrate with inhibitor, then the inhibitor is binding reversibly and competitively (it is binding to the active site rather than another site on the enzyme), as shown in Figure 5 (A). Noncompetitive inhibition, on the other hand, would produce a Lineweaver-Burk plot, Figure 5 (B), with different inhibitor concentration curves yielding the same $K_{m, app}$. Uncompetitive inhibition would yield a Lineweaver-Burk plot, Figure 5 (C), with parallel inhibitor concentrations curves. These curves have different maximum velocities and different $K_{m, app}$.

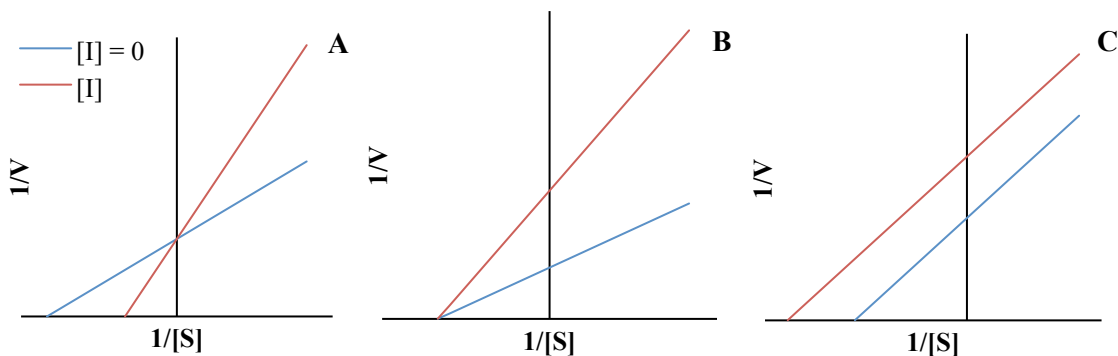
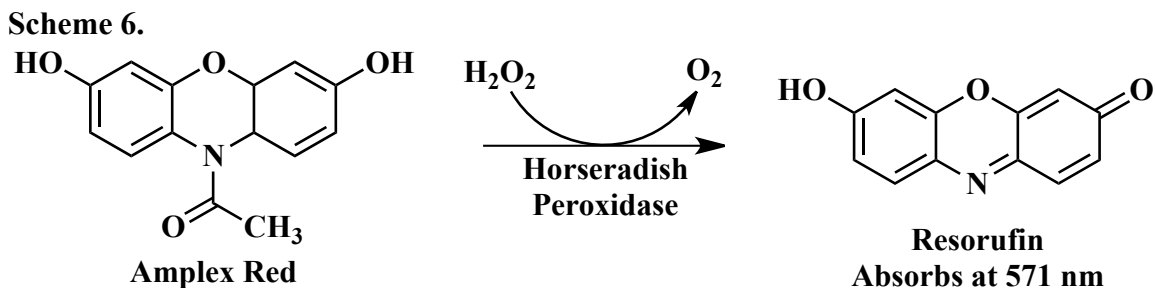


Figure 5. Lineweaver-Burk plots for (A) competitive, (B) noncompetitive, and (C) uncompetitive inhibition. A blue line corresponds to no inhibitor being present and a red line corresponds to the presence of inhibitor.

Herein, the conversion of Amplex® Red to resorufin, as shown in Scheme 6, is used to monitor the potencies of the prepared compounds.²⁹



The assay functions by coupling the production of hydrogen peroxide, produced by the enzyme's catalyzed reaction, to the conversion of Amplex® Red to a product that absorbs in the visible region of the electromagnetic spectrum, resorufin, which can then easily be monitored. The appearance of resorufin per unit of time as a function of inhibitor concentration allows for determination of potency.

1.7 Docking Analysis to Probe the Enzyme Active Site

A qualitative analysis by enzyme/inhibitor modeling can be used to determine why certain inhibitors performed better than others. Specifically, energy minimization calculations (force field calculations) via AutoDock Vina can be used in the visualization program *UCSF Chimera* to predict the most favorable binding modes for each inhibitor.³⁰ This mode can then be analyzed with respect to the amino acid residues present in the corresponding environment to theorize why certain inhibitors are better than others. Knowledge of the amino acid residues being interacted with and any favorable or unfavorable interactions can then be used for better design of MAO B inhibitors in the future. In addition, this qualitative output is accompanied by a quantitative measure. AutoDock Vina measures a docking score for each inhibitor, providing a measure of ΔG which is accompanied by a root mean square deviation (RMSD) upper bound and lower bound.³¹ The ΔG value indicates how favorable it is for the inhibitor to bind to the active

site and how spontaneous the process is, while the RMSD provides a measure of the error in the calculation. The more largely negative the ΔG value the more the binding of the inhibitor to the active site is favored. An understanding of the polar and nonpolar interactions, as well as steric interactions, occurring between an inhibitor and the active site during competitive inhibition can provide insight into structural modifications that can be made towards the production of more effective inhibitors.

This work seeks to correlate potent inhibition (K_i) with large negative docking scores, in turn, allowing for computational docking to be used to rationally predict the structures of more potent inhibitors of MAO B. These structures can then be pursued as lead compounds for enzymatic inhibition in the future.

2. Experimental

All solvents and reagents obtained from Sigma Aldrich, Fisher Science Education, Flinn Scientific, and Fluka analytical and were used without further purification. TLC was performed when denoted using silica plates. Chromatographic separations were done using silica gel and the flash methodology. NMR spectra were obtained using a JEOL 300 MHz NMR spectrometer and chloroform-*d* as solvent unless otherwise stated.

Molecular masses were acquired using an AB SCIEX TripleTOF 4600 mass spectrometer. Melting points (mp) were obtained with a Buchi Melting Point M-565 apparatus. The 96 well-plate assays were analyzed by a BMG Labtech SPECTROstar Omega spectrophotometer. The Amplex® Red Monoamine Oxidase Assay Kit (A12214) from Life Technologies was employed to perform 96 well-plate kinetic assays.²⁹

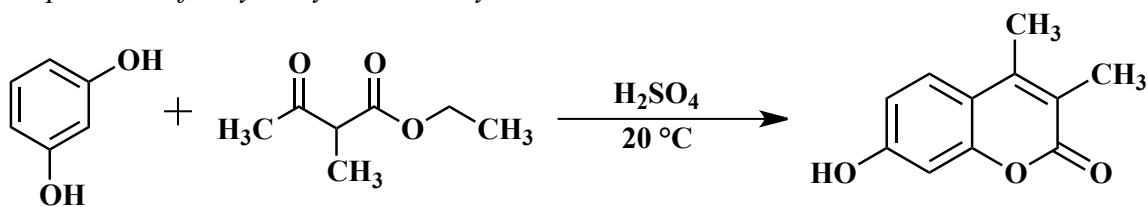
Monoamine oxidase B SUPERSOMES™ were purchased from BD Biosciences.³²

Computational docking studies were performed using AutoDock Vina calculations within the UCSF Chimera visualization program. NMR spectra for assignment reference, along with mass spectra, are located in Appendix B. ¹³C NMR spectra are included for compounds not previously reported within the literature.

2.1 Synthesis

2.1.1 Synthesis of 7-nitrobenzyloxy Substituted Coumarin Derivatives

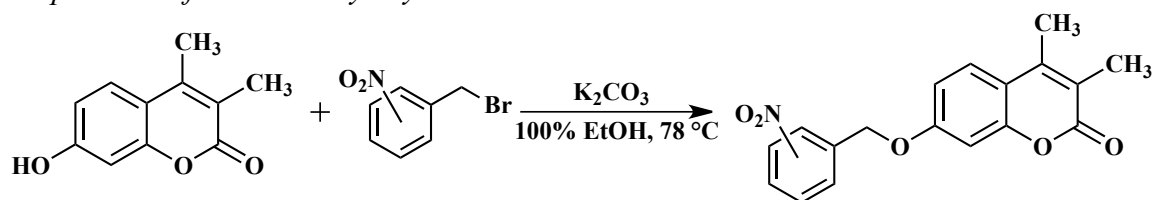
Preparation of 7-hydroxy-3,4-dimethylcoumarin^{24,33}



To a 100 mL round-bottom flask secured within an ice/NaCl bath a stir bar and 44 mL of concentrated sulfuric acid were added. The acid was then stirred while a solution

containing 4.4 g (40 mmol, 1 equiv.) of resorcinol and 5.7 mL (43 mmol, 1 equiv.) of ethyl-2-methyl acetoacetate was prepared. This solution was then added to the round-bottom flask. Stirring occurred for two hours before removal of the ice bath. The solution was left to stir overnight before being poured into a 1 L beaker containing crushed ice to the 200 mL mark and the corresponding volume of distilled water. The solution was stirred till all of the ice had melted and precipitation had begun. The solution was then cooled in an ice bath for 10 minutes. Vacuum filtration of the crude precipitated product yielded a pale white solid, which was washed three times with cold distilled water. Upon drying the obtained solid was resuspended in 34 mL of 5% sodium hydroxide. This solution was then filtered through a funnel equipped with a cotton plug and slowly stirred and acidified to pH 5 using 2 M sulfuric acid solution. The precipitating solution was placed on ice for 10 minutes before being vacuum filtered. The collected solid was redissolved in a minimal amount of hot 95% ethanol, hot filtered, and then allowed to slowly cool before being placed in an ice bath for 10 minutes. The solution was next vacuum filtered, yielding long, thin white crystals. 35% yield. The product, 7-hydroxy-3,4-dimethylcoumarin, was found in agreement with ^1H NMR assignment performed by Xie et al.³³ ^1H NMR: δ (ppm) = 9.31 (s, 1 H, *e*); 6.81 (d, 1 H, *c*); 6.11(d, 1 H, *d*); 6.01(s, 1 H, *f*); 1.70(s, 3 H, *b*); 1.48(s, 3 H, *a*) ppm.

Preparation of 7-nitrobenzyloxy substituted coumarins¹⁶

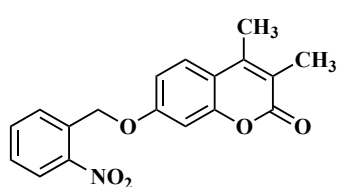


First, 0.22 g (1.3 mmol, 1 equiv.) of the appropriate 7-hydroxycoumarin derivative, 0.17 g (1.3 mmol, 1 equiv.) of anhydrous potassium carbonate, and 0.54 g (2.5 mmol, 2 equiv.) of the appropriate nitrobenzyl bromide derivative were added to a 100 mL round-bottom flask along with a stir bar. Next, 30 mL of 100% ethanol was added to the round-bottom and stirring was initiated along with heating to reflux. The solution was refluxed for four hours, then cooled to room temperature. Next, 2 mL of 1 M hydrochloric acid was added to the reaction solution in order to cause the precipitate to fall out of solution and to react any remaining carbonate. The round-bottom flask was then put in an ice-bath for 10 minutes before being vacuum filtered. The light yellow solid was then dissolved in a minimal amount of hot 95% ethanol and quickly hot filtered through a funnel equipped with a cotton plug. The warm filtrate was then allowed to cool to room temperature and was then cooled on ice for 10 minutes. After this duration the solution was vacuum filtered to yield the product.

7-(2-nitrobenzyl)oxy-4-methylcoumarin (**1**). Light yellow solid, 64% yield, mp 186.4-

187.6 °C. ¹H NMR: δ (ppm) = 8.20 (d, 1 H, *j*); 7.84 (d, 1 H, *g*); 7.69 (dd, 1 H, *h*); 7.55 (d, 1 H, *c*); 7.52 (dd, 1 H, *i*); 6.97 (d, 1 H, *d*); 6.91 (s, 1 H, *e*); 6.16 (s, 1 H, *a*); 5.61 (s, 2 H, *f*); 2.41 (s, 3 H, *b*). ¹³C NMR: δ (ppm) = 161.1 (*j*); 161.0 (*g*); 155.3 (*i*); 152.5 (*b*); 134.2 (*q*); 132.7 (*m*); 128.9 (*l*); 128.6 ppm (*n*); 125.9 (*o*); 125.4 (*e*); 125.2 (*p*); 114.4 (*a*); 112.6 (*d*); 112.4 (*f*); 102.5 (*h*); 67.4 (*k*); 18.8 (*c*). HRMS (ESI), *m/z*: calculated for C₁₇H₁₃NO₅ [M+H]⁺: 312.08, found 312.0994.

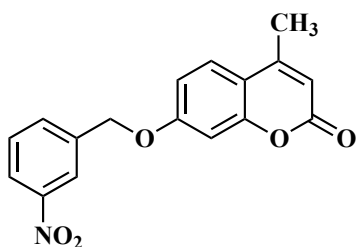
7-(2-nitrobenzyl)oxy-3,4-dimethylcoumarin (**2**). Light yellow solid, 72% yield, mp 213.8-



214.7 °C. $^1\text{H NMR}$: δ (ppm) = 8.21 (d, 1 H, *j*); 7.86 (d, 1 H, *g*); 7.69 (dd, 1 H, *h*); 7.55 (d, 1 H, *c*); 7.52 (dd, 1 H, *i*); 6.96 (d, 1 H, *d*); 6.88 (s, 1 H, *e*); 5.55 (s, 2 H, *f*); 2.37 (s, 3 H, *b*); 2.19 (s, 3 H, *a*). $^{13}\text{C NMR}$: δ (ppm) = 159.9 (*k*); 159.9 (*h*); 153.4 (*j*); 146.1 (*r*); 146.1 (*c*); 134.2 (*n*); 132.5 (*m*); 128.8 (*o*); 128.6 (*p*); 125.6 (*f*); 125.3 (*q*); 119.6 (*a*);

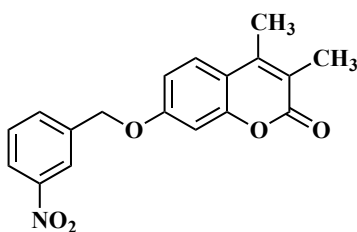
114.6 (*e*); 112.2 (*g*); 102.2 (*i*); 67.34 (*l*); 15.2 (*d*); 13.30 (*b*). HRMS (ESI), m/z : calculated for $\text{C}_{18}\text{H}_{15}\text{NO}_5$ $[\text{M}+\text{H}]^+$: 326.10, found 326.1141.

7-(3-nitrobenzyl)oxy-4-methylcoumarin (**3**).¹⁶ Light yellow solid, 99% yield, mp = 185.2-



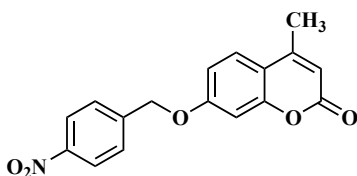
186.6 °C. $^1\text{H NMR}$: δ (ppm) = 8.33 (s, 1H, *j*); 8.21 (d, 1H, *i*); 7.76 (d, 1H, *c*); 7.60 (d, 1H, *g*); 7.53 (dd, 1H, *h*); 6.95 (d, 1H, *d*); 6.88 (s, 1H, *e*); 6.16 (s, 1H, *a*); 5.22 (s, 2H, *f*); 2.41 (s, 3H, *b*) HRMS (ESI), m/z : calculated for $\text{C}_{17}\text{H}_{13}\text{NO}_5$ $[\text{M}+\text{H}]^+$: 312.08, found 312.0981.

7-(3-nitrobenzyl)oxy-3,4-dimethylcoumarin (**4**).¹⁶ Light yellow solid, 77% yield, 194.9-



196.6 °C. $^1\text{H NMR}$: δ (ppm) = 8.33 (s, 1H, *j*); 8.20 (d, 1H, *i*); 7.76 (d, 1H, *c*); 7.59 (d, 1H, *g*); 7.51 (dd, 1H, *h*); 6.95 (d, 1H, *d*); 6.84 (s, 1H, *e*); 5.20 (s, 2H, *f*); 2.37 (s, 3H, *b*); 2.16 (s, 3H, *a*). HRMS (ESI), m/z : calculated for $\text{C}_{18}\text{H}_{15}\text{NO}_5$ $[\text{M}+\text{H}]^+$: 326.10, found 326.1140.

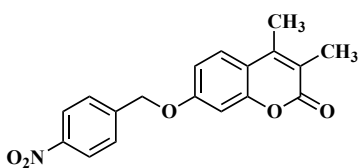
7-(4-nitrobenzyl)oxy-4-methylcoumarin (**5**). Light yellow solid, 71% yield, 204.6-206.4



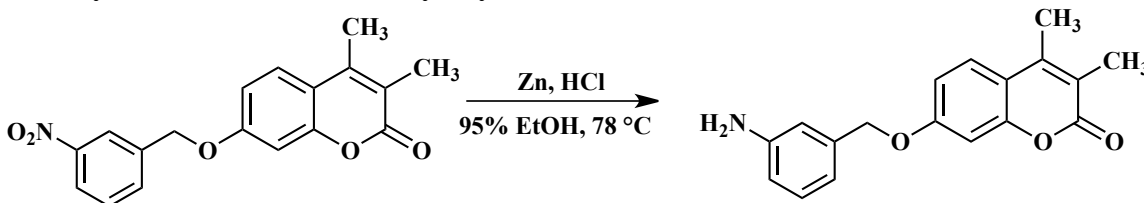
°C. $^1\text{H NMR}$: δ (ppm) = 8.26 (d, 2H, *h*); 7.55 (d, 1H, *c*); 7.52 (d, 2H, *g*); 6.95 (d, 1H, *d*); 6.86 (s, 1H, *e*); 6.17 (s, 1H, *a*); 5.24 (s, 2H, *f*); 2.41 (s, 3H, *b*). $^{13}\text{C NMR}$: δ (ppm) = 161.1 (*j*); 161.0 (*g*); 155.3 (*i*); 152.5 (*b*); 147.9 (*o*); 143.2 (*l*); 127.8 (*m*); 125.9 (*e*); 124.1 (*n*); 114.4 (*a*); 112.8 (*d*); 112.6 (*f*); 102.0 (*h*); 69.1 (*k*); 18.8 (*c*). HRMS (ESI), m/z :

calculated for $\text{C}_{17}\text{H}_{13}\text{NO}_5$ $[\text{M}+\text{H}]^+$: 312.08, found 312.0979.

7-(4-nitrobenzyl)oxy-3,4-dimethylcoumarin (**6**).¹⁶ Light yellow solid, 78% yield, mp 219.5-220.9 °C. ¹H NMR: δ (ppm) = 8.27 (d, 2H, *h*); 7.62 (d, 1H, *c*); 7.51 (d, 2H, *g*); 6.95 (d, 1H, *d*); 6.84 (s, 1H, *e*); 5.22 (s, 2H, *f*); 2.37 (s, 3H, *b*); 2.20 (s, 3H, *a*). HRMS (ESI), *m/z*: calculated for C₁₈H₁₅NO₅ [M+H]⁺: 326.10, found 326.1141.



2.1.2 Synthesis of 7-aminobenzylxy Substituted Coumarin Derivatives

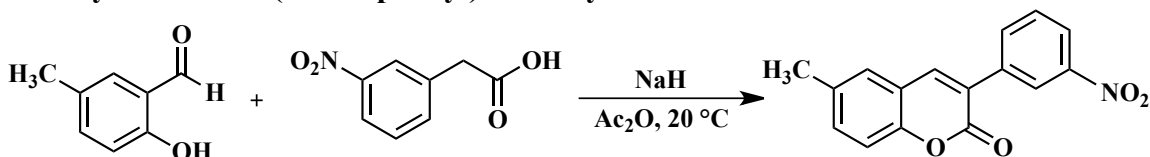


To a 100 mL round-bottom flask 0.10 g (0.34 mmol, 1 equiv.) of 7-(3-nitrobenzyl)oxy substituted coumarin, a stir bar, and 15 mL of 95% ethanol were combined. The solution was then warmed and stirred before addition of 0.15 g (2.3 mmol, 6.7 equiv.) powdered zinc and dropwise 0.4 mL concentrated hydrochloric acid. This solution was refluxed for three hours before being cooled to room temperature. The solution was then filtered and diluted with 20 mL of distilled water. Next, 5% sodium hydroxide solution was added to the reaction solution slowly, with stirring, until the pH measured neutral by litmus paper. During the addition of base a white precipitate formed. This solution was then extracted five times with 15 mL portions of ethyl acetate. Sodium chloride and additional ethyl acetate were added in the case that an emulsion formed during the aqueous work-up. The isolated organic phase was then dried over anhydrous magnesium sulfate and evaporated to yield a light yellow solid. The collected solid was recrystallized from 100% ethanol. Analysis by ¹H NMR in chloroform-*d* revealed the structure of the target compound.

7-(3-aminobenzyl)oxy-4-methylcoumarin (**7**). White crystals, 14% yield, mp 150.3-152.1 °C. ¹H NMR: δ (ppm) = 7.48 (d, 1H, *c*); 7.15 (dd, 1H, *h*); 6.90 (d, 1H, *g*); 6.88 (s, 1H, *k*); 6.75 (d, 1H, *d*); 6.72 (s, 1H, *e*); 6.65 (d, 1H, *i*); 6.13 (s, 1H, *a*); 5.04 (s, 2H, *f*); 3.70 (br, 2H, *j*); 2.39 (s, 3H, *b*). ¹³C NMR: δ (ppm) = 161.8 (*j*); 161.4 (*g*); 155.3 (*i*); 152.6 (*b*); 146.9 (*n*); 137.1 (*l*); 129.8 (*p*); 125.6 (*e*); 117.3 (*q*); 115.1 (*m*); 113.9 (*o*); 113.0 (*a*); 112.1 (*d*); 110.5 (*f*); 102.1 (*h*); 70.6 (*k*); 18.8 (*c*). HRMS (ESI), *m/z*: calculated for C₁₇H₁₅NO₃ [M+H]⁺: 282.11, found 282.1236.

7-(3-aminobenzyl)oxy-3,4-dimethylcoumarin (**8**).¹⁶ White crystals, 14% yield, mp 183.5-184.2 °C. ¹H NMR: δ (ppm) = 7.48 (d, 1H, *c*); 7.17 (dd, 1H, *h*); 6.92 (d, 1H, *g*); 6.87 (s, 1H, *k*); 6.81 (d, 1H, *d*); 6.75 (s, 1H, *e*); 6.65 (d, 1H, *i*); 5.03 (s, 2H, *f*); 3.71 (br, 2H, *j*); 2.36 (s, 3H, *b*); 2.18 (s, 1H, *a*). HRMS (ESI), *m/z*: calculated for C₁₈H₁₇NO₃ [M+H]⁺: 296.12, found 296.1395.

2.1.3 Synthesis of 3-(3-nitrophenyl)-6-methylcoumarin



To a 10 mL round-bottom flask 0.25 g (1.8 mmol, 1 equiv.) 2-hydroxy-5-methylbenzaldehyde, 0.33 g (1.8 mmol, 1 equiv.) 3-nitrophenylacetic acid, and stir bar were added. Next, the flask was capped, evacuated, and purged with argon before the addition of 2.0 mL (21 mmol, 21 equiv.) of acetic anhydride. The flask was again capped, evacuated, and purged with argon. Stirring was initiated. Next, 0.16 g (4.0 mmol, 4 equiv.) sodium hydride (60% dispersion in mineral oil) was then added to the solution in small portions before the reaction was capped and allowed to stir for three hours. The reaction was monitored by thin layer chromatography using 1:9 ethyl acetate: hexane as solvent. After this time the reaction was gravity filtered to remove solid. The solid was washed with ethyl acetate and the filtrate was then extracted with three 20 mL portions of 5% sodium bicarbonate. The organic phase was then dried over anhydrous magnesium

sulfate before being gravity filtered into a 100 mL round-bottom flask. To the round-bottom flask 1 g of silica gel was added. The solution was then evaporated. Flash chromatography (1:9 ethyl acetate: hexane) was performed to obtain the desired compound, 3-(3-nitrophenyl)-6-methylcoumarin (**9**), which was recrystallized from 100% ethanol to yield a white solid. 5% yield. ^1H NMR of this compound was in agreement with findings of Matos et al.³⁴ mp 240.9-241.2 °C. ^1H NMR: δ (ppm) = 8.55 (s, 1H, *e*); 8.27 (d, 1H, *b*); 8.14 (d, 1H, *d*); 7.89 (s, 1H, *a*); 7.66 (t, 1H, *c*); 7.41 (s, 1H, *f*); 7.38 (d, 1H, *i*); 7.28 (d, 1H, *h*); 2.44 (s, 3H, *g*). HRMS (ESI), m/z : calculated for $\text{C}_{16}\text{H}_{11}\text{NO}_4$ $[\text{M}+\text{H}]^+$: 282.07, found 282.0868.

2.2 Enzyme Inhibition Kinetics

Substrate concentrations tested were 0.5, 1.0, 1.5, 2.0, and 2.5 mM. The substrate utilized was tyramine. These concentrations were prepared by pipetting the appropriate volume of 100 mM stock substrate solution to each well. Three inhibitor stock solutions were prepared to yield final inhibitor concentrations of 4, 8, and 12 nM in the 200 μL well-plate volume. These concentrations were produced by preparing stock solutions of 10 mg of inhibitor dissolved in 1 mL of dimethyl sulfoxide (DMSO). The stock solution was then serially diluted to yield concentrations of 100, 200, and 300 nM solutions. 8 μL of this dilution was pipetted to yield final concentration of 5% DMSO in the well-plate. This concentration of DMSO was shown not to impact MAO activity.²³ The total volume of each well was 200 μL and 0.004 mg of human MAO B was placed in each well. A 0.05 M, pH 7.4 sodium phosphate buffer was used to constitute substrate and enzyme, as

well as Amplex® Red and horseradish peroxidase. The final concentrations of Amplex® Red and horseradish peroxidase were 400 μ M and 2 U/mL, respectively.

First, 8 μ L of inhibitor solution, yielding 4, 8, or 12 nM final concentrations in 200 μ L final volume, was pipetted into each respective well of the 96-well plate. The assay should observe each substrate concentration at each inhibitor concentration, as well as the substrate tested with no inhibitor present. Next, 100 μ L of Amplex® Red reagent (containing horseradish peroxidase) was added to each well followed by 42 μ L of the appropriate concentration of substrate dissolved in buffer. Lastly, a total volume of 0.8 μ L of enzyme was added to 49.2 μ L of buffer. To initiate the reaction this volume of enzyme-buffer, 50 μ L, was added to each well using a multi-well pipetter. The well-plate was then placed in the well-plate reader for one hour with data acquisition every minute. Absorbance measurements were made at 571 nm. A standard curve, Beer's law plot, of the reaction product, resorufin, was prepared in order to quantify of the amount of reaction product, resorufin, being produced by the enzyme during the assay. Lineweaver-Burk plots were then constructed in order to determine inhibitor K_i values.

2.3 Inhibitor Docking Experiments

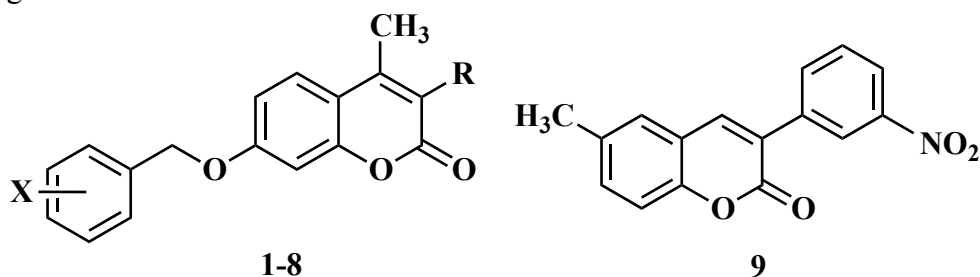
Inhibitor docking was performed after first importing the PDB crystal structure of MAO B and subsequently preparing a ligand (inhibitor) for docking. Next, Dock Prep was run to prepare the ligand and receptor for docking. AutoDock Vina was then run with receptor search volume center of 50 x 160 x 30 Å and a size of 18 x 18 x 18 Å, which includes the active site cavity and entrance cavity of MAO B. Docking scores selected were those with RMSD upper bound and lower bound values of zero. Contact

parameterization involved a Van der Waal overlap $\geq -0.4 \text{ \AA}$ with 0.0 being subtracted from potentially hydrogen bonding pairs. Contact pairs four or fewer bonds apart were ignored.

3. Results

The structures of the compounds prepared in this study are summarized in Table 1 alongside their experimentally determined K_i values and computationally determined docking scores.

Table 1. Results of inhibition kinetics for nine prepared compounds with respective docking scores.



Compound	X ^a	R ^a	Average K_i (nM) ^b	Docking Score (kcal/mol)
1	<i>o</i> -NO ₂	H	11.7 ^c	-2.8
2	<i>o</i> -NO ₂	CH ₃	4.9 ± 2.0	-2.0
3	<i>m</i> -NO ₂	H	10.4 ± 1.3	-3.2
4	<i>m</i> -NO ₂	CH ₃	10.7 ± 2.7	-2.4
5	<i>p</i> -NO ₂	H	4.4 ± 2.0	-1.8
6	<i>p</i> -NO ₂	CH ₃	1.3 ± 0.5	-1.7
7	<i>m</i> -NH ₂	H	9.4 ± 1.4	-3.8
8	<i>m</i> -NH ₂	CH ₃	2.4 ± 1.4	-2.7
9	Shown Above		1.3 ± 1.3	-3.8

a – Substitution patterns for 7-benzyloxy substituted coumarins.

b – ± values indicate range associated with K_i , not standard deviation.

c – Only one inhibitor concentration plotted, no range attainable.

The average K_i value was determined by averaging K_i values obtained at different concentrations of the same inhibitor. Because the sample size of inhibitor concentrations for each respective inhibitor was deemed not sufficiently large, the standard deviation association with these values was not reported. Rather, a range about the average K_i was reported to give insight into the range in the determined K_i values. The correlation between the K_i values and respective docking scores of the 7-nitrobenzyloxy substituted coumarins is shown in Figure 6.

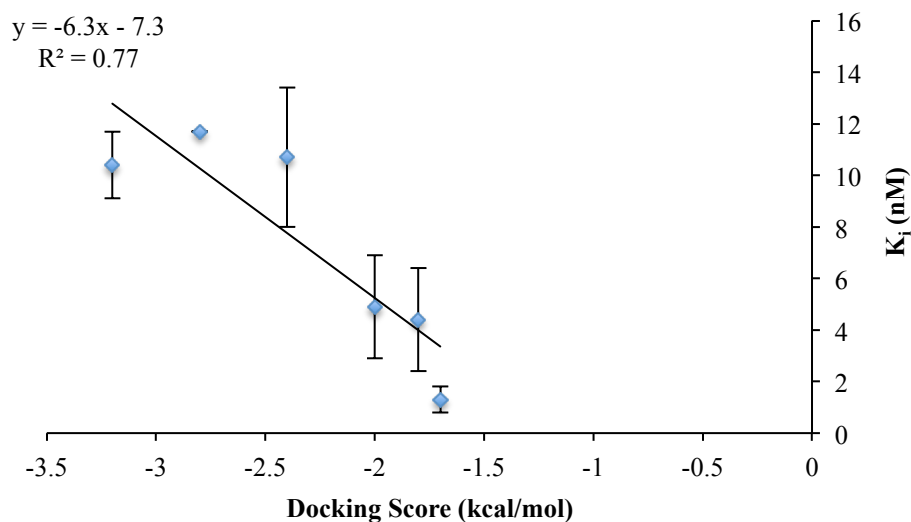


Figure 6. Correlation between the inhibition constant, K_i , for 7-nitrobenzyloxy substituted coumarins and their respective docking scores.

K_i values were extracted from Lineweaver-Burk plots shown in Figures 7-15.

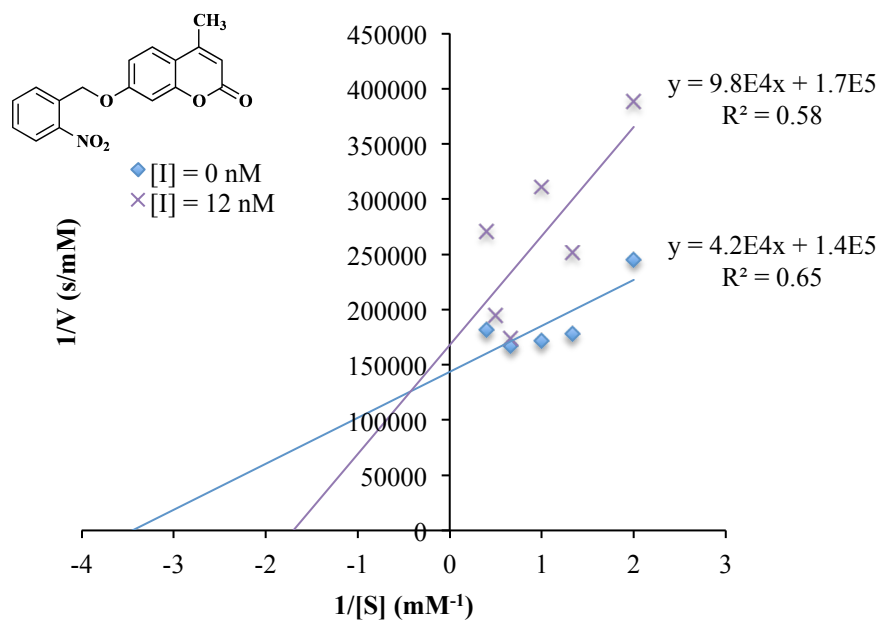


Figure 7. Lineweaver-Burk plot of one concentration of 7-(2-nitrobenzyl)oxy-4-methylcoumarin inhibiting MAO B.

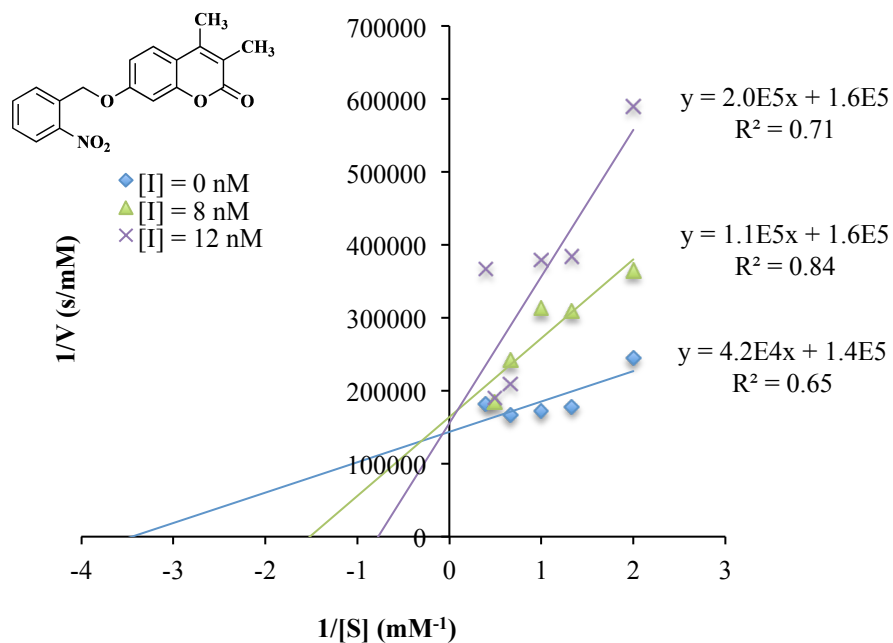


Figure 8. Lineweaver-Burk plot of two different concentrations of 7-(2-nitrobenzyl)oxy-3,4-dimethylcoumarin inhibiting MAO B.

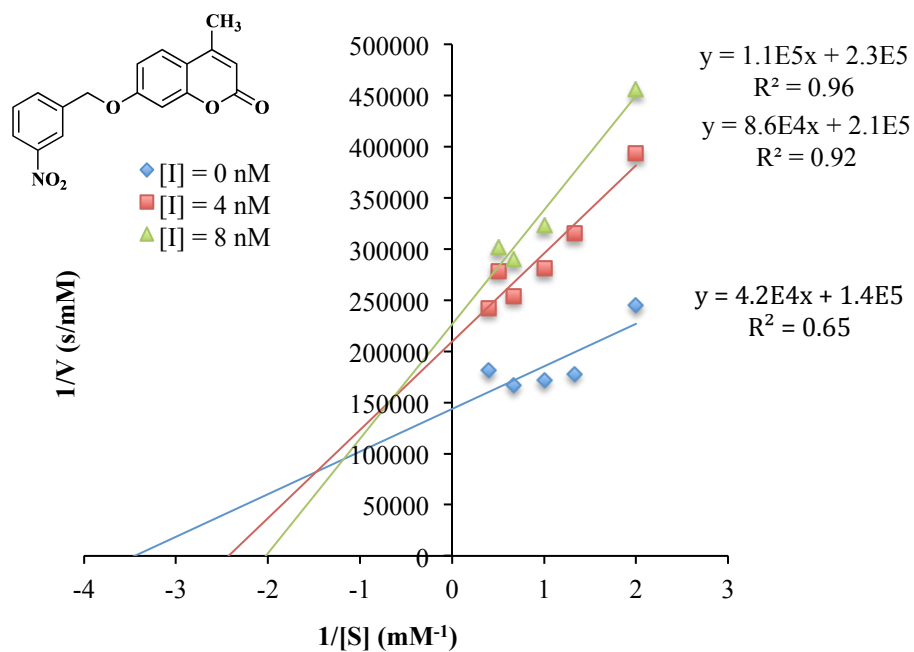


Figure 9. Lineweaver-Burk plot of two different concentrations of 7-(3-nitrobenzyl)oxy-4-methylcoumarin inhibiting MAO B.

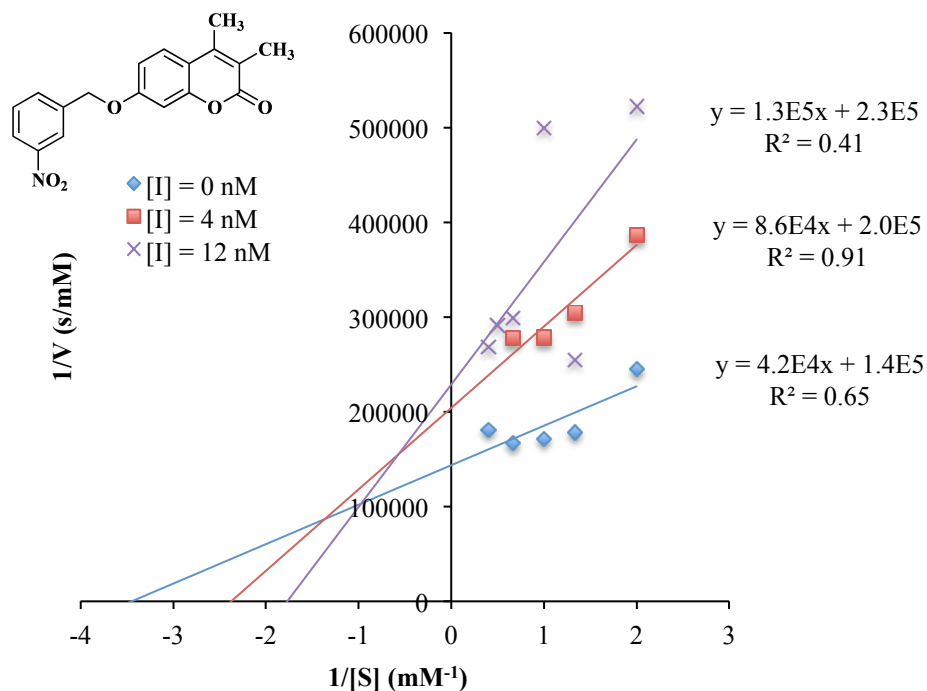


Figure 10. Lineweaver-Burk plot of two different concentrations of 7-(3-nitrobenzyl)oxy-3,4-dimethylcoumarin inhibiting MAO B.

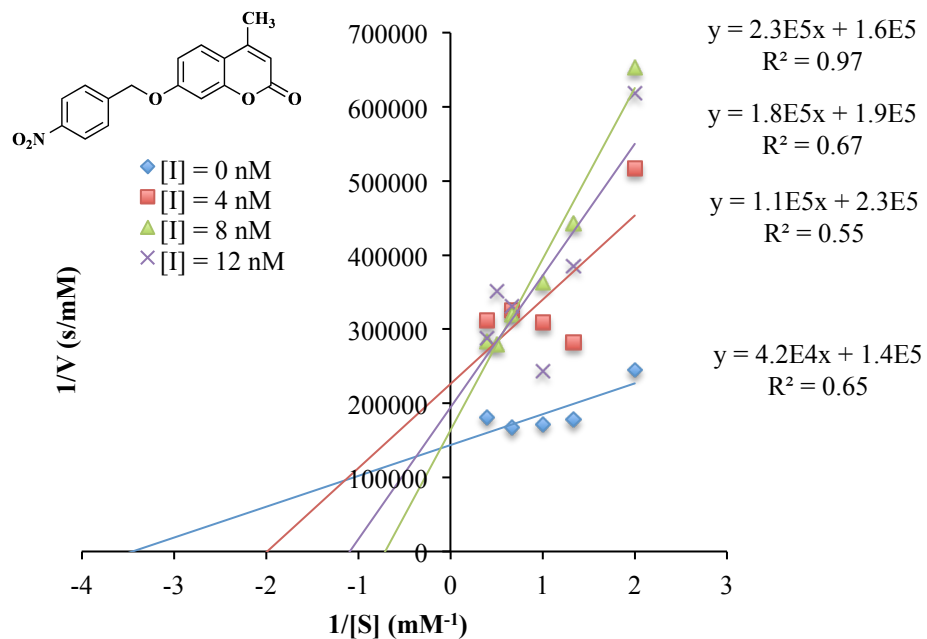


Figure 11. Lineweaver-Burk plot of three different concentrations of 7-(4-nitrobenzyl)oxy-4-methylcoumarin inhibiting MAO B.

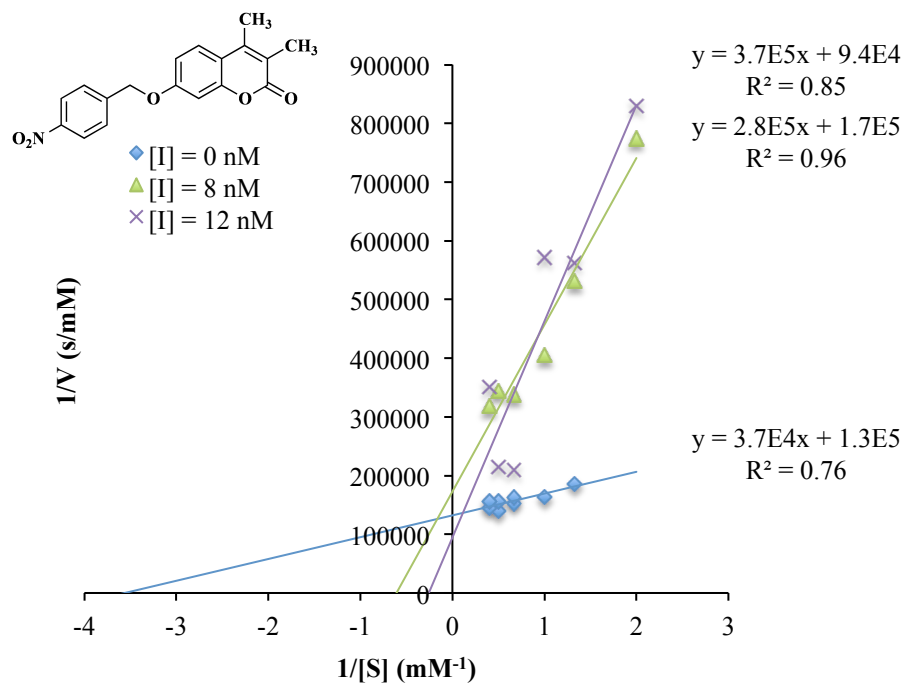


Figure 12. Lineweaver-Burk plot of two different concentrations of 7-(4-nitrobenzyl)oxy-3,4-dimethylcoumarin inhibiting MAO B.

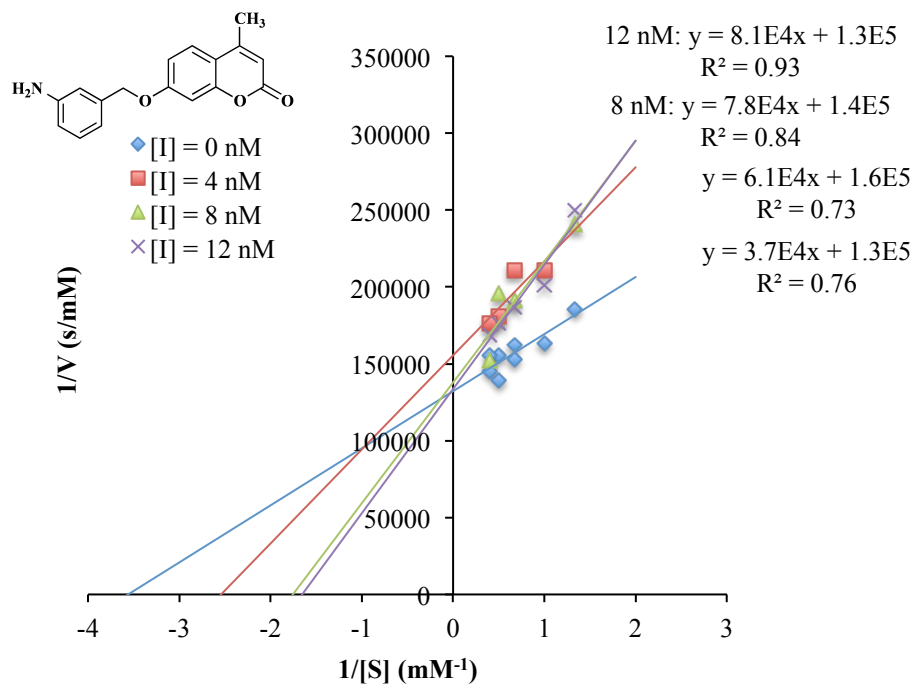


Figure 13. Lineweaver-Burk plot of three different concentrations of 7-(3-aminobenzyl)oxy-4-methylcoumarin inhibiting MAO B.

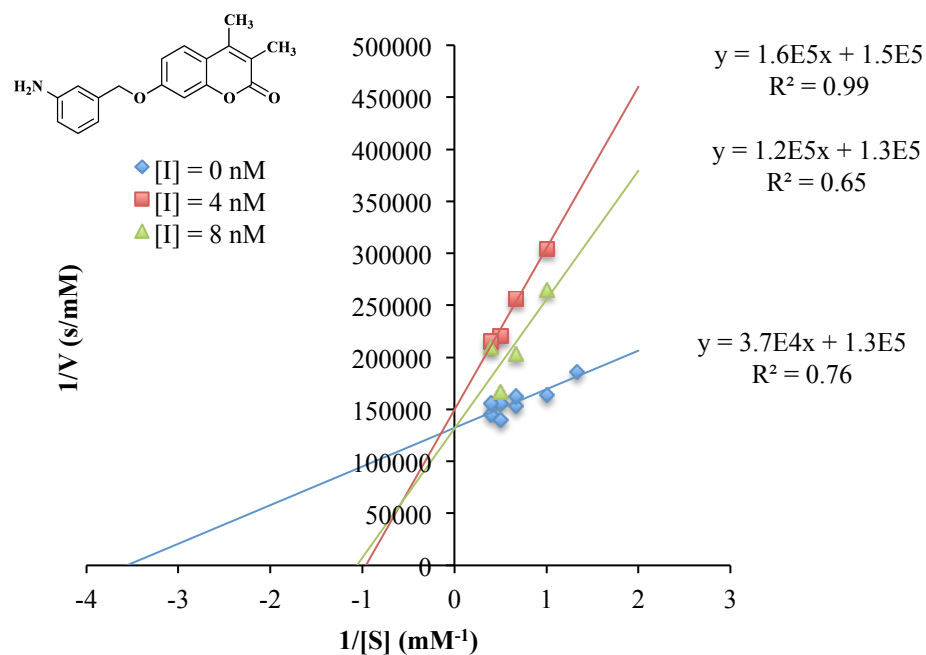


Figure 14. Lineweaver-Burk plot of two different concentrations of 7-(3-aminobenzyl)oxy-3,4-dimethylcoumarin inhibiting MAO B.

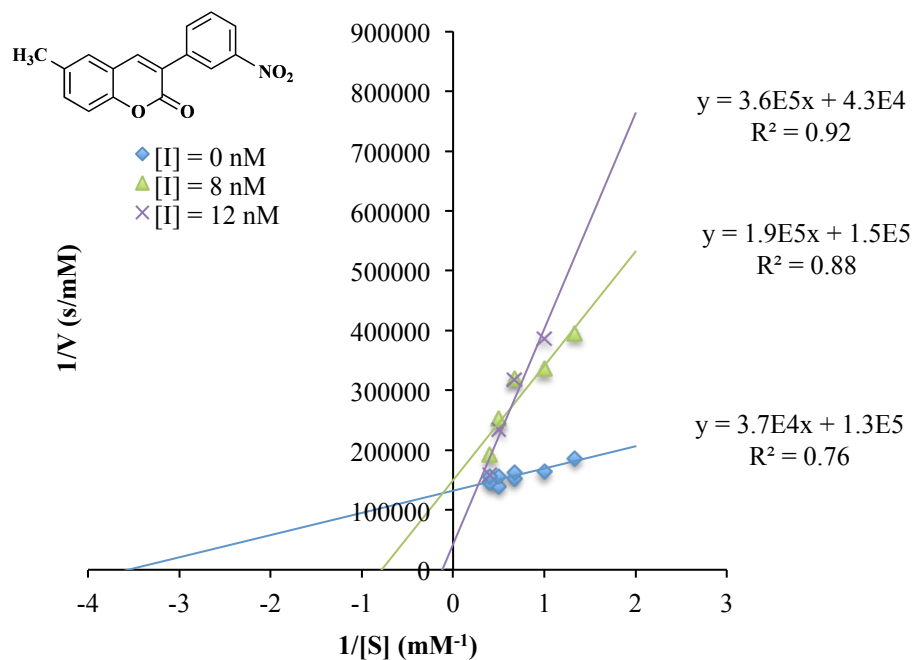


Figure 15. Lineweaver-Burk plot of three different concentrations of 3-(3-nitroaryl)-6-methylcoumarin inhibiting MAO B.

The activity plot for MAO B at the highest substrate concentration tested, 2.5 mM, is shown in Figure 16. The concentration values contained in the activity plot were produced using the Beer's Law plot for resorufin at 571 nm, Figure 17.

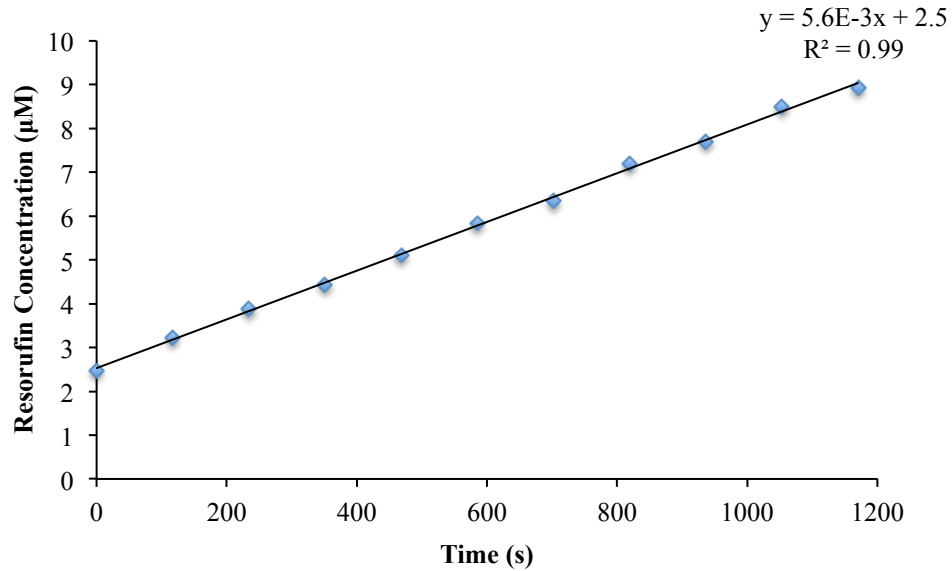


Figure 16. MAO B activity plot at substrate concentration of 2.5 mM over 20 minutes.

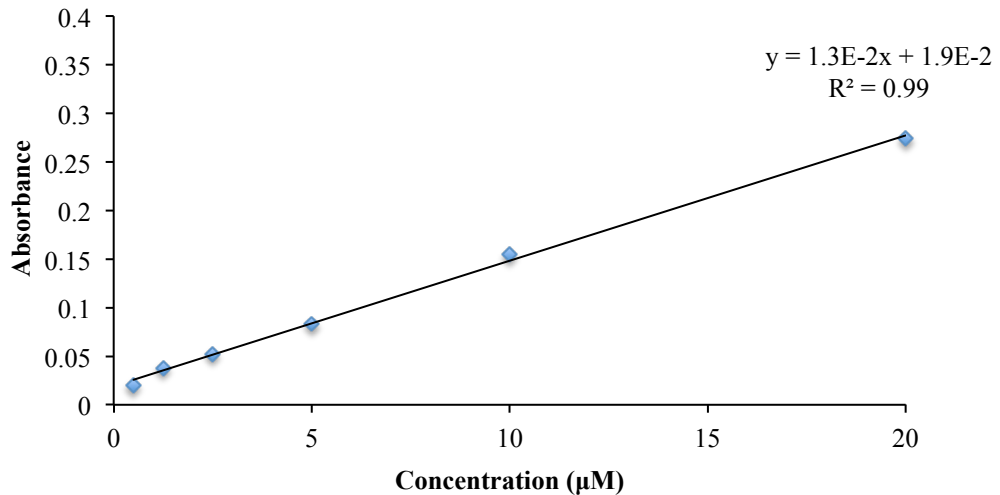


Figure 17. Beer's law plot for resorufin at 571 nm.

4. Discussion

4.1 Synthesis

Preparation of 7-hydroxy-3,4-dimethylcoumarin, Scheme 2, was successful, resulting in 35% yield. Synthesis of 7-nitrobenzyloxy substituted coumarins, Scheme 3, afforded the six predicted products in good yield, 64-99%. 7-hydroxy-3,4-dimethylcoumain was used to prepare compounds **2**, **4**, and **6**, while commercially available 7-hydroxy-4-methylcoumarin (Sigma Aldrich) was used to prepare inhibitors **1**, **3**, and **5**. Reduction of these compounds, Scheme 4, to their corresponding amine derivatives was only successful for *meta*-substituted derivatives, compounds **7** and **8**, and acquired yields were low, 14% for both compounds. Attempted reaction methodology for this transformation can be found in Appendix A. Synthesis of 3-nitroaryl substituted coumarins, Scheme 5, was successful for the preparation of the 3-(3-nitrophenyl)-6-methylcoumarin, **9**, which was acquired in low yield (5%). Attempts to synthesize the *ortho*- and *para*- substituted derivatives were not successful. Addition of acetic acid during the course of the reaction should produce the corresponding *ortho*- and *para*-substituted derivatives, as well as the *meta*- substituted coumarin derivative, in good yield.³⁴

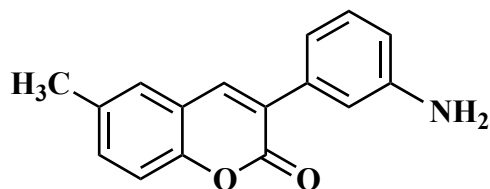
4.2 Kinetics and Docking Scores

The results of kinetics experiments indicated that the prepared inhibitors bind reversibly and competitively (differing $K_{m, app.}$, but same maximum velocity) to the enzyme active site. In addition, inhibition was observed to be potent, with K_i values in the nanomolar range. The kinetic data illustrated that 3,4-dimethyl substitution of the

coumarin provided more potent inhibition than 4-methyl substitution. This result is important because previously it was shown that 3,4-dimethyl substitution enhanced inhibitor selectivity towards MAO B.¹⁶ In addition, from Table 1 it can be noted that *para*-nitro substitution in 7-(4-nitrobenzyl)oxy-3,4-dimethylcoumarin, compound **6**, enhanced inhibitor potency to a K_i value of 1.3 ± 0.5 nM. *meta*-amino substitution in 7-(3-aminobenzyl)oxy-3,4-dimethylcoumarin, compound **8**, provided potent inhibition at a K_i of 2.4 ± 1.4 nM. Perhaps most noteworthy of these potent inhibitors was 3-(3-nitrophenyl)-6-methylcoumarin, compound **9**, with the largest substituent in the 3-position (phenyl ring) and K_i of 1.3 ± 1.3 nM.

Linear correlation was observed between the kinetically determined K_i values for the 7-nitrobenzyloxy substituted coumarins and their computationally determined docking scores, Figure 6. This correlation, however, indicated that a low K_i value (potent inhibition) corresponded to a less negative docking score (less favorable inhibitor binding), which is the opposite correlation that would be expected. This opposite correlation could be attributed to AutoDock Vina not parameterizing the docking calculation accurately with respect to experimental findings. In reality enzymes are not rigid structures and their amino acid residues move, but AutoDock Vina treats enzymes as rigid molecules. Additional hydrogen bonding of an inhibitor to the active site can occur when residues are flexible. Because AutoDock Vina does not observe these interactions in its calculation there exists inherent flaws in the binding affinity determination. The docking calculation could also have performed poorly for the structural changes exhibited in the 7-nitrobenzyloxy substituted coumarins due to the relatively small changes made in their structures. For example, AutoDock Vina does not take into account hydrogen bond

directionality, which could be an important factor for distinguishing between 7-nitrobenzyloxy substituted coumarin binding affinities.³¹ A more sophisticated docking calculation that takes into account ab initio calculations, as well as force field calculations could potentially provide better correlation with K_i values. Ultimately, experimental data is more meaningful than the docking calculations and a larger, more negative docking score should intuitively correspond to potent inhibition. This is corroborated by Matos et al. who prepared 3-(3-aminophenyl)-6-methylcoumarin and showed that its inhibition was more potent than that of 3-(3-nitrophenyl)-6-methylcoumarin, compound **9**.³⁴ Docking of 3-(3-aminophenyl)-6-methylcoumarin, Figure 18, produced a docking score of -5.3 kcal/mol (more largely negative than -3.8 kcal/mol for 3-(3-nitrophenyl)-6-methylcoumarin).



**Predicted
Docking Score: -5.3 kcal/mol**

Figure 18. Docking score calculated for 3-(3-aminophenyl)-6-methylcoumarin.

This compound was originally predicted to be a more potent inhibitor than 3-(3-nitrophenyl)-6-methylcoumarin based upon the docking image of the most stable conformation, Figure 19.

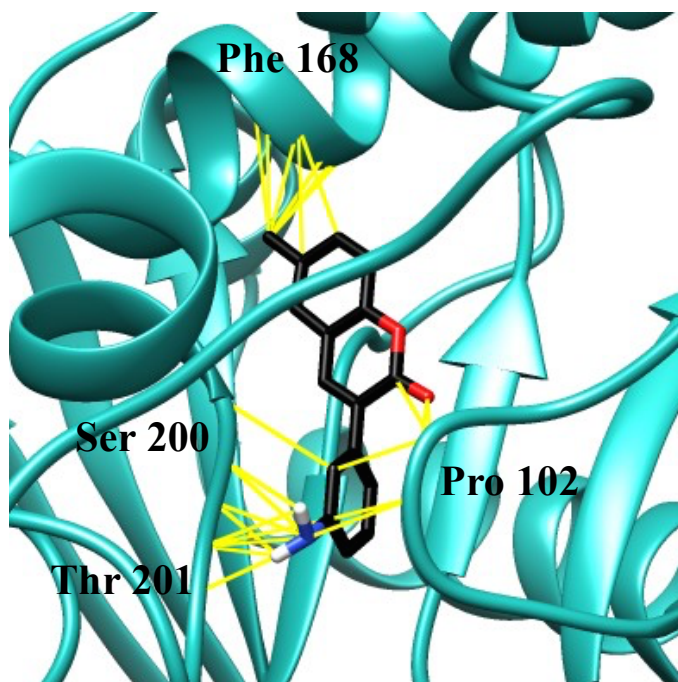


Figure 19. Docking of 3-(3-aminophenyl)-6-methylcoumarin to MAO B.

The image displays hydrogen bonding and polar intermolecular interactions with the nitro substituent and amino acid residues Ser 200, Thr 201, and Pro 102 of the entrance cavity and active site cavity. It was postulated that amino substitution would provide better binding of the inhibitor because it can receive and donate a hydrogen bond while the nitro group can only receive a hydrogen bond. Assuming that more largely negative docking scores correlate to more potent inhibition, the established docking protocol should be able to predict more potent inhibitor structures.

Analysis of several prepared complexes docking to MAO B, Figures 20-22, revealed that intermolecular interactions and steric collisions with Phe 168, Pro102, Thr 201, and Ser 200 were significant to coumarin binding.

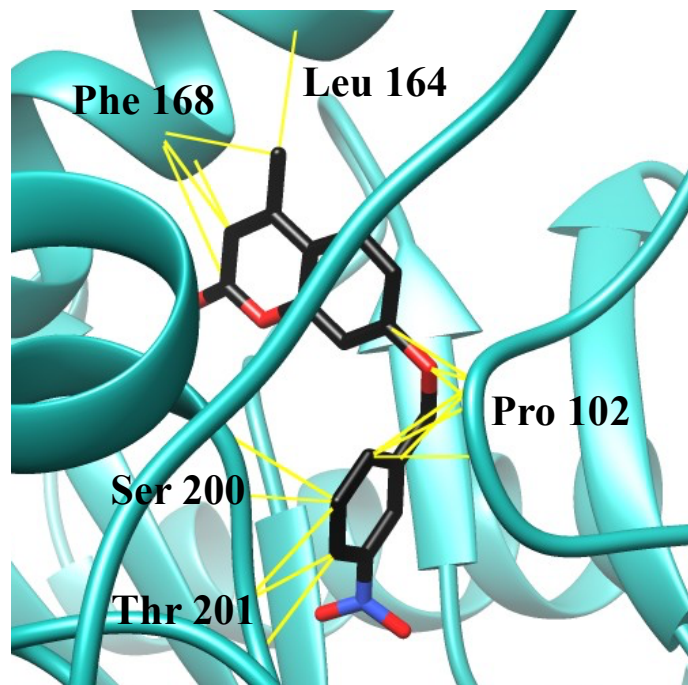


Figure 20. Docking of 7-(3-nitrobenzyl)oxy-4-methylcoumarin to MAO B.

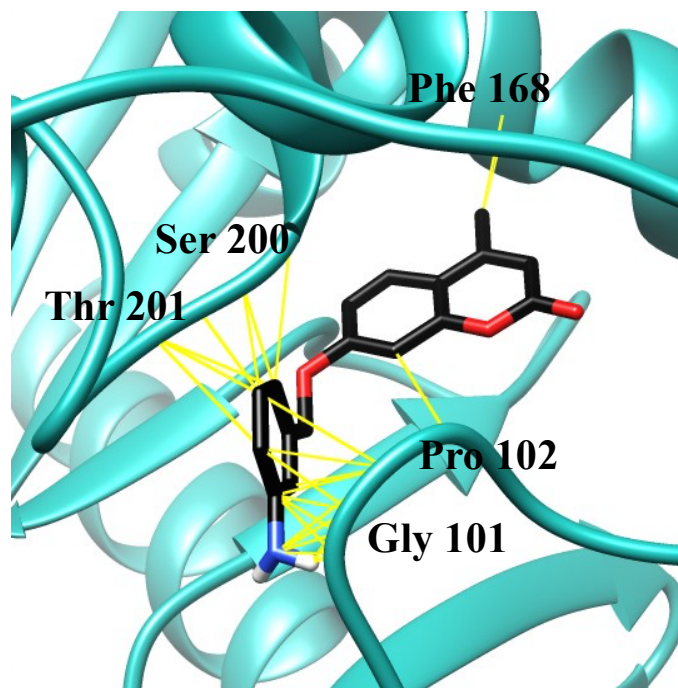


Figure 21. Docking of 7-(3-aminobenzyl)oxy-4-methylcoumarin to MAO B.

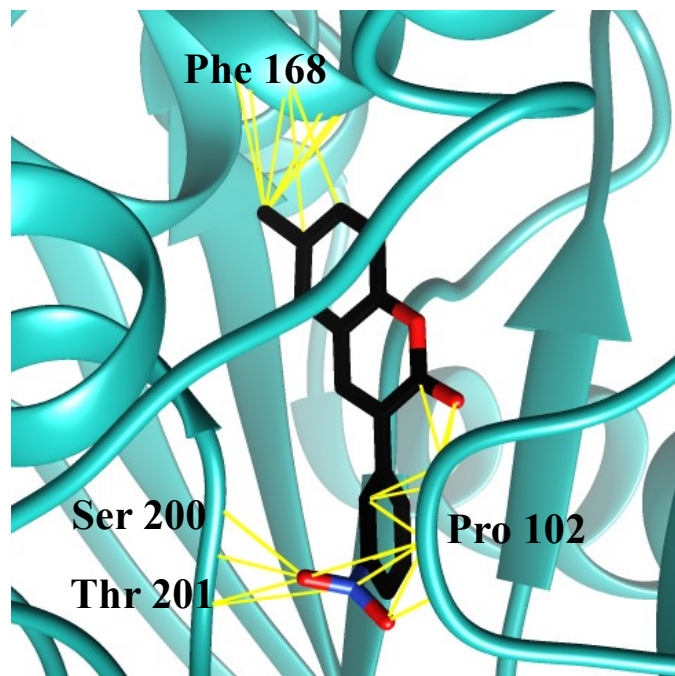


Figure 22. Docking of 3-(3-nitrophenyl)-6-methylcoumarin to MAO B.

It appears that the coumarin plays more of a structural role as scaffold for its bound substituents which possess larger interactions with the residues of the active site, than as a primary source for binding to the active site. Enhancement of the interactions observed between coumarin-bound substituents with the residues of the active site allowed for more potent inhibitors to be designed.

4.3 More Potent Inhibitor Structure Predictions

With the docking protocol's accuracy verified the inhibitor's binding interactions within the active site were examined more closely. It was noted that docking of 3-(3-aminophenyl)-6-methylcoumarin could be improved by replacing the 6-methyl substitution, which was likely sterically clashing with Phe 168, with a substitution that could participate in hydrogen bonding, such as a hydroxyl group. The 3-(3-

aminophenyl)-6-hydroxycoumarin was docked to MAO B, as shown in Figure 23, and was found to have a docking score of -5.8 kcal/mol.

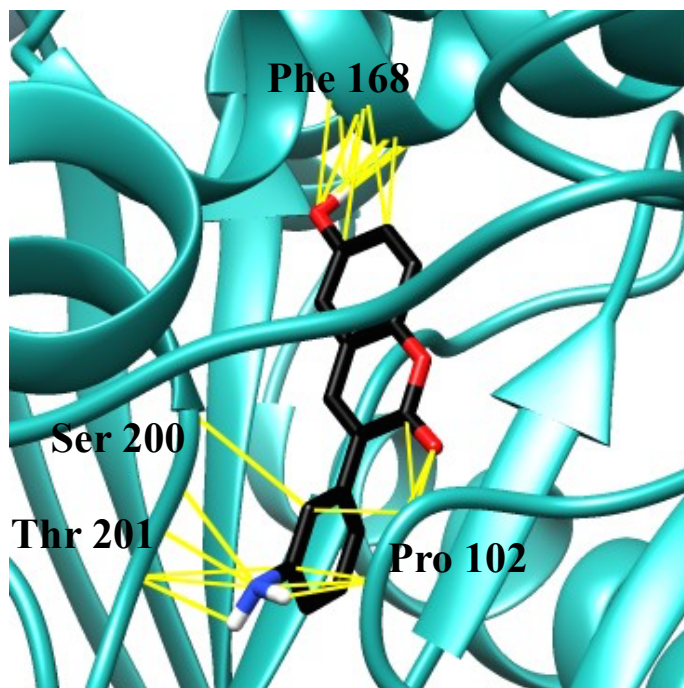


Figure 23. Docking of 3-(3-aminophenyl)-6-hydroxycoumarin to MAO B.

This docking score was more largely negative than that of 3-(3-aminophenyl)-6-methylcoumarin, -5.3 kcal/mol, indicating that it likely binds to MAO B with even greater potency.

Further diversification of this promising scaffold involved replacement of the 6-hydroxyl group with 6-amino substitution and altering the 3-aminophenyl substitution to 3-hydroxyphenyl substitution, as shown in Figure 24.

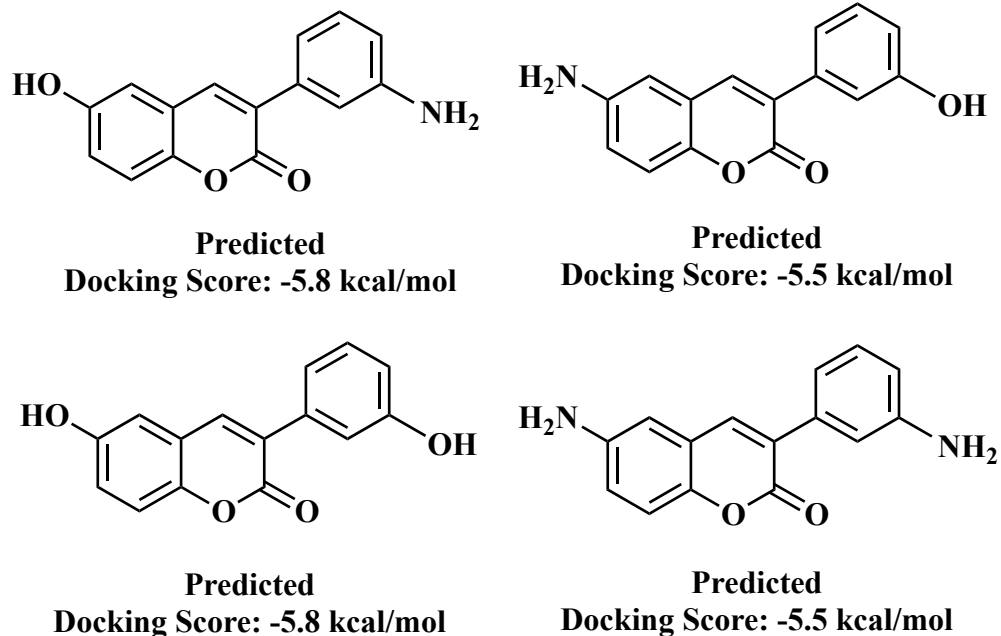


Figure 24. Docking scores of several coumarins with structures analogous to 3-(3-aminophenyl)-6-hydroxycoumarin were found to be more potent computationally than 3-(3-aminophenyl)-6-methylcoumarin.

Overall, based on docking scores, it appeared that modification of 6-hydroxy substitution to 6-amino substitution was not as favorable. This is likely because the increased size of the amino substituent causes more steric clashes than a hydroxyl substituent does, causing less favorable binding. This finding is supported by the findings of Matos et al.²² On the other hand, converting the 3-aminophenyl substituent to a 3-hydroxyphenyl substituent was found to not impact the docking score. This could be because steric clashes at the 3-aryl substituent are not as significant as they are at the 6- position of the coumarin.

The 3-(3-aminophenyl)-6-hydroxycoumarin and its analogues could prove to be important leads for further study in the pursuit of coumarin-based MAO B inhibitors, as identified by this study. To determine if 3-(3-aminophenyl)-6-hydroxycoumarin (docking

score -5.8 kcal/mol) is actually a more potent inhibitor than 3-(3-aminophenyl)-6-methylcoumarin (docking score -5.3 kcal/mol) the compound should be prepared synthetically and assayed to determine its potency. These compounds could likely be prepared by methodology analogous to that utilized by Kabeya et al. to prepare 3-(3-hydroxyphenyl)-6-hydroxycoumarin by use of the appropriately substituted reagents.³⁵

5. References

1. Strolin-Benedetti, M.; Tipton, K. F.; Whomsley, R. Amine Oxidases and Monoxygenases in the In Vivo Metabolism of Xenobiotic Amines in Humans: Has the Involvement of Amine Oxidases Been Neglected? *Fundam. Clin. Pharmacol.* **2007**, *21*, 467–479.
2. Youdim, M. B.; Bakhle, Y. S. Monoamine Oxidase: Isoforms and Inhibitors in Parkinson's Disease and Depressive illness. *J. Pharmacol.* **2006**, *147*, 287–296.
3. Yamada, M.; Yasuhara, H. Clinical Pharmacology of MAO Inhibitors: Safety and Future. *Neurotox.* **2004**, *25*, 215-221.
4. Patil, P. O.; Bari, S. B.; Firke, S. D.; Deshmukh, P. K.; Donda, S. T.; Patil, D. A. A Comprehensive Review on Synthesis and Designing Aspects of Coumarin Derivatives as Monoamine Oxidase Inhibitors for Depression and Alzheimer's Disease. *Bioorg. Med. Chem.* **2013**, *21*, 2434-2450.
5. Sayre, L. M.; Perry, G.; Smith, M. A. Oxidative Stress and Neurotoxicity. *Chem. Res. Toxicol.* **2008**, *21*, 172–188.
6. Walker, W. H.; Kearney, E. B.; Seng, R.; and Singer, T. P. The Covalently-Bound Flavin of Hepatic Monoamine Oxidase 2. Identification and Properties of Cysteinyl Riboflavin. *Eur. J. Biochem.* **1971**, *24*, 328.
7. Olanow, C. W.; Hauser, R. A.; Jankovic, J.; Langston, W.; Lang, A.; Poewe, W.; Tolosa, E.; Stocchi, F.; Melamed, E.; Eyal, E.; Rascol, O. A. Randomized, Double-Blind, Placebo-Controlled, Delayed Start Study To Assess Rasagiline as a Disease Modifying Therapy in Parkinson's Disease (the ADAGIO Study): Rationale, Design, and Baseline Characteristics. *Movement Disord.* **2008**, *23*, 2194– 2201.
8. Bach, A. W.; Lan, N. C.; Johnson, D. L.; Abell, C. W.; Bembenek, M. E.; Kwan, S. W.; Seeburg, P. H.; Shih, J. C. cDNA Cloning of Human Liver Monoamine Oxidase A and B: Molecular Basis of Differences in Enzymatic Properties. *Proc. Natl. Acad. Sci. U.S.A.* **1988**, *85*, 4934–4938.
9. Binda, C.; Wang, J.; Pisani, L.; Caccia, C.; Carotti, A.; Salvati, P.; Edmondson, D. E.; Mattevi, M. Structures of Human Monoamine Oxidase B Complexes with Selective Noncovalent Inhibitors: Saffinamide and Coumarin Analogs. *J. Med. Chem.* **2007**, *50*, 5848– 5852.
10. De Colibus, L.; Li, M.; Binda, C.; Lustig, A.; Edmondson, D. E.; Mattevi, A. Three-Dimensional Structure of Human Monoamine Oxidase A (MAO A): Relation to the Structures of Rat MAO A and Human MAO B. *Proc. Natl. Acad. Sci. U.S.A.* **2005**, *102*, 12684–12689.

11. Binda, C.; Hubálek, F.; Li, M.; Edmondson, D. E.; Mattevi, A. Crystal Structure of Human Monoamine Oxidase B, a Drug Target Enzyme Monotopically Inserted into the Mitochondrial Outer Membrane. *FEBS Letters*. **2004**, 564, 225-228.
12. Binda, C.; Newton-Vinson, P.; Hubálek, F.; Edmondson, D. E.; Mattevi, A. Structure of Human Monoamine Oxidase B, a Drug Target for the Treatment of Neurological Disorders. *Nat. Struct. Mol. Biol.* **2002**, 9, 22–26.
13. Binda, C.; Li, M.; Hubálek, F.; Restelli, N.; Edmondson, D. E.; Mattevi, A. Insights into the Mode of Inhibition of Human Mitochondrial Monoamine Oxidase B from High-Resolution Crystal Structures. *Proc. Natl. Acad. Sci. U.S.A.* **2003**, 100, 9750–9755.
14. Pisani, L.; Barletta, M.; Soto-Otero, R.; Nicolotti, O.; Mendez-Alvarez, E.; Catto, M.; Introcaso, A.; Stefanachi, A.; Cellamare, S.; Altomare, C.; Carotti, A. Discovery, Biological Evaluation, and Structure–Activity and –Selectivity Relationships of 6'-Substituted (*E*)-2-(Benzofuran-3(2*H*)-ylidene)-*N*-methylacetamides, a Novel Class of Potent and Selective Monoamine Oxidase Inhibitors. *J. Med. Chem.* **2013**, 56, 2651-2664.
15. Geha, R. M.; Rebrin, I.; Chen, K.; Shih, J. C. Substrate and Inhibitor Specificities for Human Monoamine Oxidase A and B are Influenced by a Single Amino Acid. *J. Biol. Chem.* **2001**, 276, 9877– 9882.
16. Gnerre, C.; Catto, M.; Leonetti, F.; Weber, P.; Carrupt, P.-A.; Altomare, C.; Carotti, A.; Testa, B. Inhibition of Monoamine Oxidase by Functionalized Coumarin Derivatives: Biological Activities, QSAR, and 3D-QSARs. *J. Med. Chem.* **2000**, 43, 4747– 4758.
17. Coulson, C.J. The Inactivation of Monoamine Oxidase by Clorgyline. *Biochem Pharmacol.* **1969**, 18, 1447.
18. Thull, U.; Carrupt, P.A.; Testa, B.; Pargyline Analogues as Potent, Non-selective Monoamine Oxidase Inhibitors. *Pharm. Pharmacol. Commun.* **1998**, 4, 579-581.
19. Pisani, L.; Muncipinto, G.; Miscioscia, T. F.; Nicolotti, O.; Leonetti, F.; Catto, M.; Caccia, C.; Salvati, P.; Soto-Otero, R.; Mendez-Alvarez, E.; Passeleu, C.; Carotti, A. Discovery of a Novel Class of Potent Coumarin Monoamine Oxidase B Inhibitors: Development and Biopharmacological Profiling of 7-[(3-Chlorobenzyl)oxy]-4-[(methylamino)methyl]-2*H*-chromen-2-one Methanesulfonate (NW-1772) as a Highly Potent, Selective, Reversible, and Orally Active Monoamine Oxidase B Inhibitor. *J. Med. Chem.* **2009**, 52, 6685-6706.
20. Shih, J.C.; Chen, K.; Ridd, M.J. Monoamine Oxidase: From Genes to Behavior. *Annu. Rev. Neurosci.* **1999**, 22, 197-217.
21. Sahoo, A.; Yabanoglu, S.; Sinha, B. N.; Ucar, G.; Basu, A.; Jayaprakash, V. Towards Development of Selective and Reversible Pyrazoline Based MAO-Inhibitors: Synthesis, Biological Evaluation and Docking Studies. *Bioorg. Med. Chem. Lett.* **2010**, 20, 132.

22. Matos, M.J.; Terañ, C.; Pérez-Castil, Y.; Uriarte, E.; Santana, L.; Viña, D. Synthesis and Study of a Series of 3-Arylcoumarins as Potent and Selective Monoamine Oxidase B Inhibitors *J. Med. Chem.* **2011**, 54, 7127–7137.
23. Kürti, L.; Czakó, B. Perkin Reaction. Strategic Applications of Named Reactions in Organic Synthesis, Academic Press, Burlington, 1st ed., **2005**, 338.
24. Furniss, B. S.; Hannaford, A. J.; Smith, P. W. J.; Tatchell A.R. Cognate Preparation. 4-methyl-7-hydroxycoumarin. Vogel's Text book of Practical Organic Chemistry, Pearson Education, Singapore, 5th ed., **1989**, 1193.
25. Kürti, L.; Czakó, B. Williamson Ether Synthesis. Strategic Applications of Named Reactions in Organic Synthesis, Academic Press, Burlington, 1st ed., **2005**, 484.
26. Kürti, L.; Czakó, B. Perkin Reaction. Strategic Applications of Named Reactions in Organic Synthesis, Academic Press, Burlington, 1st ed., **2005**, 338.
27. Matos, M.J.; Pérez-Cruz, F.; Vazquez-Rodriguez, S.; Uriarte, E.; Santana, L.; Borges, F.; Olea-Azar, C.; Remarkable Antioxidant Properties of a Series of Hydroxy-3-arylcoumarins. *Bioorg. & Med. Chem.* **2013**, 21, 3900-3906.
28. Cheng, Y.; Prusoff, W. H. Relationship Between the Inhibition Constant (K_i) and the Concentration of Inhibitor which Causes 50 Per Cent Inhibition (I_{50}) of an Enzymatic Reaction. *Biochem. Pharmacol.* **1973**, 22, 3099-3108.
29. Amplex® Red Monoamine Oxidase Assay Kit (A12214). *Molecular Probes.* **2004**.
30. Pettersen, E. F.; Goddard, T. D.; Huang, C. C.; Couch, G. S.; Greenblatt, D. M.; Meng, E. C.; Ferrin, T. E. UCSF Chimera – A Visualization System for Exploratory Research and Analysis. *J. Comput. Chem.* **2004**, 25, 1605-1612.
31. Trott, O.; Olson, A. J. AutoDock Vina: Improving the Speed and Accuracy of Docking with a New Scoring Function, Efficient Optimization and Multithreading. *J. Comput. Chem.* **2010**, 32, 455-461.
32. Human Monoamine Oxidase B (MAO-B) SUPERSOMES™. BD Biosciences – Discovery Labware. **2013**.
33. Xie, L.; Guo, H.; Lu, H.; Zhuang, X.; Zhang, A.; Wu, G.; Ruan, J.; Zhou, T.; Yu, D.; Qian, K.; Lee, K.; Jiang, S. Development and Preclinical Studies of Broad-Spectrum Anti-HIV Agent (3'R,4'R)-3-Cyanomethyl-4-methyl-3',4'-di-O-(S)-camphanoyl-(+)-cis-khallactone (3-Cyanomethyl-4-methyl-DCK). *J. Med. Chem.* **2008**, 51, 7689-7696.

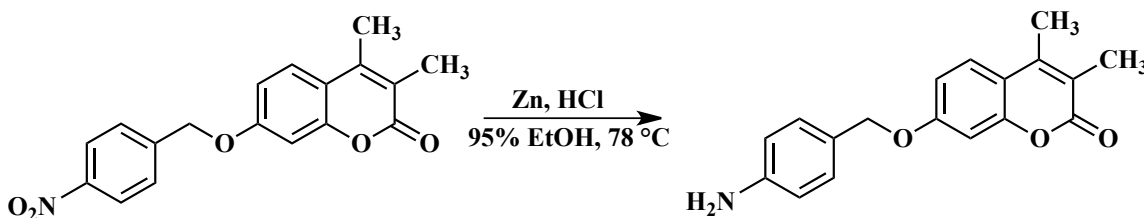
34. Matos, M. J.; Rodríguez-Enríquez, F.; Vilar, S.; Santana, L.; Uriarte, E.; Hripcsak, G.; Estrada, M.; Rodríguez-Franco, M. I.; Viña, D. Potent and Selective MAO-B Inhibitory Activity: Amino- versus Nitro-3-arylcoumarin Derivatives. *Bioorg. Med. Chem. Lett.* **2015**, *25*, 642-648.

35. Kabeya, L. M.; de Marchi, A. A.; Kanashiro, A.; Lopes, N. P.; da Silva, C. H. T. P.; Pupo, M. T.; Lucisano-Valim, Y. M. Inhibition of Horseradish Peroxidase Catalytic Activity by New 3-phenylcoumarin Derivatives: Synthesis and Structure-Activity Relationships. *Bioorg. Med. Chem.* **2007**, *15*, 1516-1524.

Appendix A. Attempted Synthetic Methodology

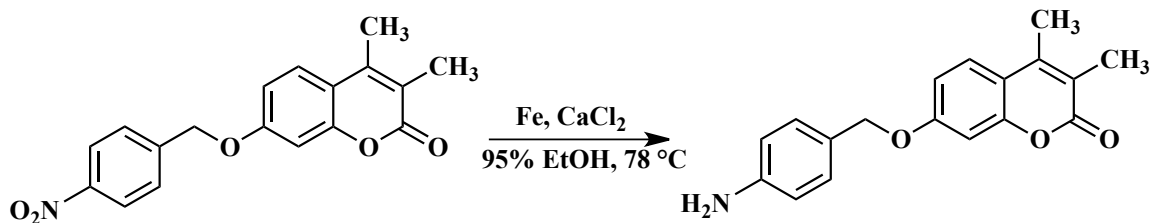
A.1 Preparation of 7-(4-aminobenzyl)oxy Substituted Coumarins

Zinc Mediated Reduction

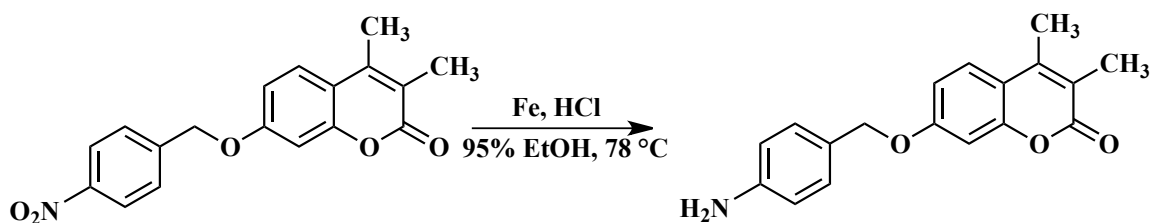


To a 100 mL round-bottom flask 0.10 g (0.30 mmol, 1 equiv.) of 7-(4-nitrobenzyl)oxy-3,4-dimethylcoumarin, a stir bar, and 15 mL of 95% ethanol were combined. The solution was then warmed with stirring before addition of 0.15 g (2.3 mmol, 6.7 equiv.) powdered zinc and dropwise 0.4 mL concentrated hydrochloric acid. This solution was refluxed for three hours before being cooled to room temperature. The solution was then filtered and diluted with 20 mL of distilled water. Next, 5% sodium hydroxide solution was added to the reaction solution slowly with stirring until the pH measured neutral by litmus paper. This solution was then extracted five times with 15 mL portions of ethyl acetate. Sodium chloride and additional ethyl acetate was added in the case that an emulsion formed during the aqueous work-up. The isolated organic phase was then dried over anhydrous magnesium sulfate and evaporated to yield a light yellow solid. The collected solid was dissolved in a minimal amount of warm 100% ethanol, then cooled on ice for 10 minutes and collected by vacuum filtration. Analysis by ¹H NMR in chloroform-*d*, with two drops of DMSO-*d*₆ to aid in solubility, revealed the structure of the isolated product was not that of the target.

Iron Mediated Reduction



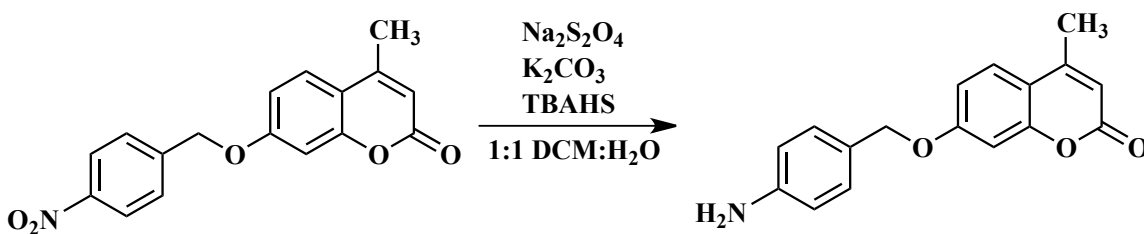
To a 100 mL round-bottom flask 0.10 g (0.30 mmol, 1 equiv.) of 7-(4-nitrobenzyl)oxy-3,4-dimethylcoumarin was added with a stir bar. Next, 20 mL of 95% ethanol was added to the flask and the solution was warmed. When the temperature approached that of reflux 50 mg (0.90 mmol, 3 equiv.) of iron filings and 0.45 g (0.3 mmol, 1 equiv.) of calcium chloride dihydrate were added to the solution. The solution was then refluxed, with stirring, for 30 minutes before TLC was taken (1:1 ethyl acetate:hexane) which revealed that no reaction was occurring.



To a 100 mL round-bottom flask 0.15 g (0.46 mmol, 1 equiv.) of 7-(4-nitrobenzyl)oxy-3,4-dimethylcoumarin was added with stir bar and 20 mL of 95% ethanol. The solution was next warmed to near reflux before the addition of 90 mg (1.6 mmol, 1 equiv.) of iron filings. To the solution 0.5 mL of concentrated hydrochloric acid was then added dropwise. The solution was then refluxed for three hours before being cooled to room temperature and filtered. Next, 20 mL of distilled water was added to the filtrate for dilution. Next, 5% sodium hydroxide solution was slowly added to the reaction solution with stirring until the pH measured neutral by litmus. During this

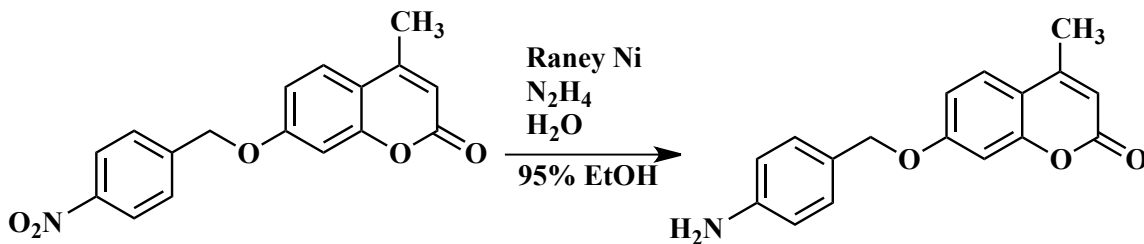
addition the solution turned from yellow to dark blue and a brown precipitate began to form. Five extractions with 15 mL portions of ethyl acetate were then performed and the organic phase was dried over anhydrous magnesium sulfate. The solvent was evaporated to yield a light yellow solid. This solid was then recrystallized from 100% ethanol, yielding a yellow solid. Analysis by ^1H NMR using chloroform- d , with two drops of DMSO- d_6 added to aid in solubility, revealed the isolated product was not the target compound.

Phase Transfer Catalyst Mediated Reduction



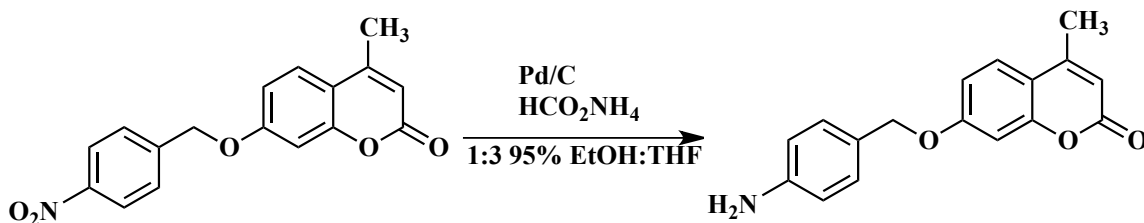
To a 25 mL round-bottom flask 33 mg (0.10 mmol, 2 equiv.) of 7-(4-nitrobenzyl)oxy-4-methylcoumarin was added with stir bar and 5 mL of dichloromethane. Next, 5 mL of distilled water was added to the flask along with 18 mg (0.053 mmol, 1 equiv.) of tertbutylammonium hydrogen sulfate, 0.10 g (0.72 mmol, 14 equiv.), and 0.10 g (0.58 mmol, 12 equiv.) sodium dithionite. A septum was then quickly placed in the mouth of the flask and pierced with a needle with a balloon attached. The solution was then stirred for 48 hours before TLC in 1:1 ethyl acetate:hexane was taken. TLC indicated that the starting material was still present and that no product had formed.

Raney Nickel Mediated Reduction



To a 250 mL round-bottom flask 50 mg (0.16 mmol, 1 equiv.) of 7-(4-nitrobenzyl)oxy-4-methylcoumarin was added along with a stir bar and 100 mL of 95% ethanol. Stirring was then initiated. Next, 0.05 mL (1.0 mmol, 6.3 equiv.) of hydrazine hydrate followed by 0.7 mL of Raney nickel was added to the reaction vessel. The reaction stirred for 30 minutes at 70 °C before being brought to 100 °C. Once the vapors of the solution indicated a neutral pH on litmus paper the reaction solution was allowed to cool to room temperature. Next, 1 mL of 2 M hydrochloric acid was added to the solution and three extractions were performed with 20 mL portions of ethyl acetate. The aqueous phase was then made pH 6 by addition of 10% sodium hydroxide. Three more extractions with 20 mL portions of ethyl acetate were performed at this point. The organic phase was then dried over anhydrous sodium sulfate and evaporated in order to yield a light brown oil. Analysis of the product by ¹H NMR, using chloroform-*d* as solvent, revealed that the isolated product was not the desired product.

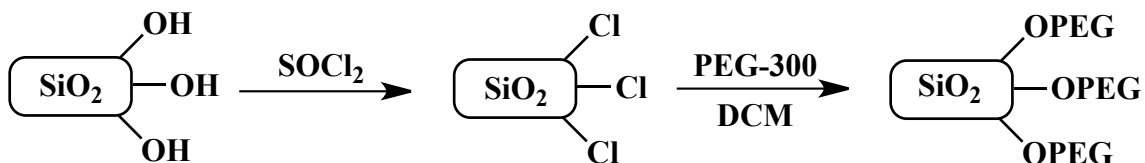
Palladium on Carbon Mediated Reduction



In a 100 mL round-bottom flask 10 mL of 95% ethanol, 30 mL of tetrahydrofuran, a stir bar, and 50 mg (0.16 mmol, 1 equiv.) 7-(4-nitrobenzyl)oxy-4-methylcoumarin were combined. The solution was stirred while 0.12 g (1.9 mmol, 12 equiv.) of ammonium formate followed by 57 mg (0.53 mmol, 3.3 equiv.) of 10% Palladium on carbon were quickly added. The mouth of the flask was then quickly fit with a septum, which was pierced by a needle with balloon attached. The solution was stirred for two hours while being monitored by TLC (1:1 ethyl acetate: hexane). At this point in time the reaction was found to be complete, so the reaction solution was then filtered through a funnel equipped with celite pad above a cotton plug. The filtered solution was then evaporated to yield a light yellow oil. Analysis of this product in chloroform-*d* by ¹H NMR revealed that the collected product was not the desired product.

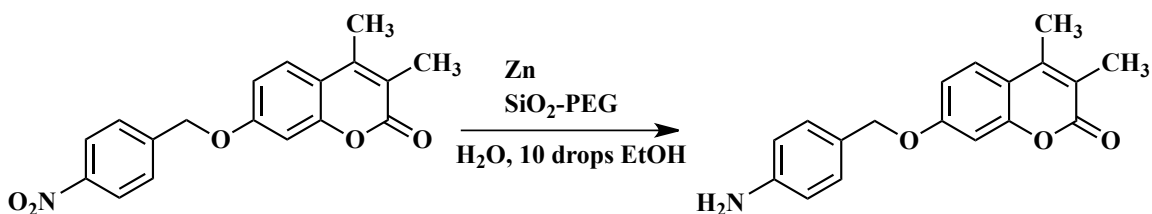
Zinc and PEG immobilized on Silica Mediated Reduction

Polyethylene glycol was first immobilized on silica gel before the reduction of 7-(nitrobenzyl)oxy-3,4-dimethylcoumarin was attempted.



First, 1 g of silica gel was heated and allowed to cool four times under vacuum before being placed in a 10 mL round-bottom flask, evacuated with argon prior to addition, with spin vane. A septum was then fitted to the mouth of the flask and the flask was placed under an argon atmosphere and stirring was initiated. Next, 2.4 mL (33 mmol) of thionyl chloride was added to the reaction flask by syringe dropwise. The flask was then stirred for four hours before being transferred to a distillation apparatus with 50 mL of bleach in the distillate collection flask. The reaction flask was then heated to 75 °C in order to drive off all excess thionyl chloride. This flask containing the reaction product, a light brown powder – silica chloride, was then stored under argon.

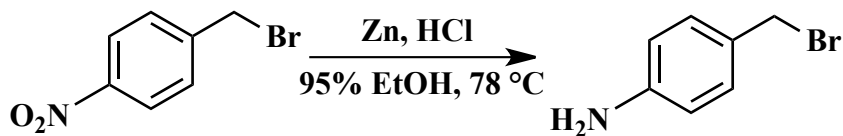
Next, 0.2 g of silica chloride was combined with 0.4 mL of dry dichloromethane and a stir bar in a 10 mL round-bottom flask under argon atmosphere. Stirring was then initiated and 0.09 mL poly(ethylene glycol)-300 was added by syringe dropwise. This reaction was stirred for two hours before being vacuum filtered. The collected solid, a light brown/grey solid – PEG immobilized on silica – was then washed with acetone three times and stored.



In order to perform the desired reduction 0.10 g (0.30 mmol, 1 equiv.) of 7-(4-nitrobenzyl)oxy-4-methylcoumarin was combined with 0.035 g of PEG immobilized on silica in a 25 mL round bottom flask with stir bar. Next, 5 mL of distilled water and 3 mL of 100% ethanol were added to the round bottom, followed by 0.22 g (3.3 mmol, 11 equiv.) of powdered zinc. The solution was then heated to reflux for two hours, allowed to continue to stir at room temperature for 18 hours, then allowed to reflux again for two hours. After this time the reaction solution was filtered and made acidic with 1 M hydrochloric acid. The solution was then extracted three times with 15 mL ethyl acetate. Next, the aqueous phase was brought to pH 6 by addition of 5% sodium hydroxide. The solution was again extracted three times with 15 mL portions of ethyl acetate. The collected organic phase was then dried over anhydrous sodium sulfate before being evaporated. Analysis of the product, a brown solid, by ^1H NMR in chloroform-*d* revealed the collected product was not the desired product.

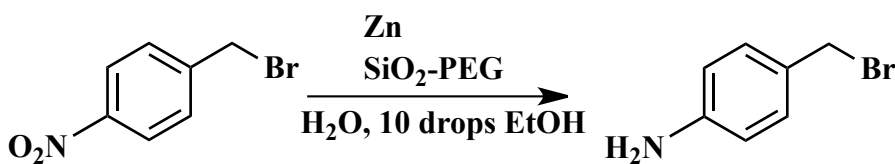
Coupling of 4-aminobenzyl bromide to 7-hydroxy-4-methylcoumarin

4-aminobenzyl bromide was prepared before the desired reaction was attempted.



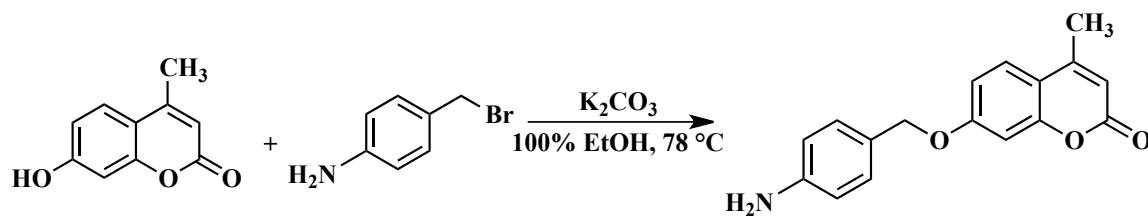
First, 76 mg (0.34 mmol, 1 equiv.) of 4-nitrobenzyl bromide was dissolved in 18 mL of warm 95% ethanol in a 100 mL round-bottom flask equipped with a star bar. Next,

0.22 g (3.3 mmol, 10 equiv.) of powdered zinc was added to the round-bottom followed by the dropwise addition of 0.5 mL of concentrated hydrochloric acid. The reaction was then refluxed with stirring for 30 minutes. TLC (1:1 ethyl acetate:hexane) at this time revealed that the reaction was complete. The flask was then cooled to room temperature before being diluted with 10 mL of distilled water. Next, the solution was brought to pH 6 by addition of 5% sodium hydroxide. Three 15 mL ethyl acetate extractions were then performed. The organic phase was then dried over anhydrous magnesium sulfate before being filtered and evaporated. The collected product was a brown/red solid. Analysis of the product by ^1H NMR in chloroform-*d* revealed that the collected product was not the desired product.



In a 10 mL round-bottom flask 0.22 g (1 mmol, 1 equiv.) of 4-nitrobenzyl bromide, a spin vane, and 5 mL of distilled water were combined. The solution was then warmed with stirring and 0.72 g (11 mmol, 11 equiv.) of powdered zinc and 0.1 g of silica supported PEG were added. After one hour the reaction was checked with TLC (1:5 tetrahydrofuran:hexane) and found to be complete. Next, the solution was allowed to cool to room temperature and filtered. The filtrate was next acidified to pH 1 by addition of 1 M hydrochloric acid. The solution was then extracted with three 20 mL portions of dichloromethane. The aqueous phase was then brought to pH 6 by addition of 10% sodium hydroxide. This solution was then extracted five times with 20 mL portions of diethyl ether. The organic phase was then dried over anhydrous sodium sulfate and

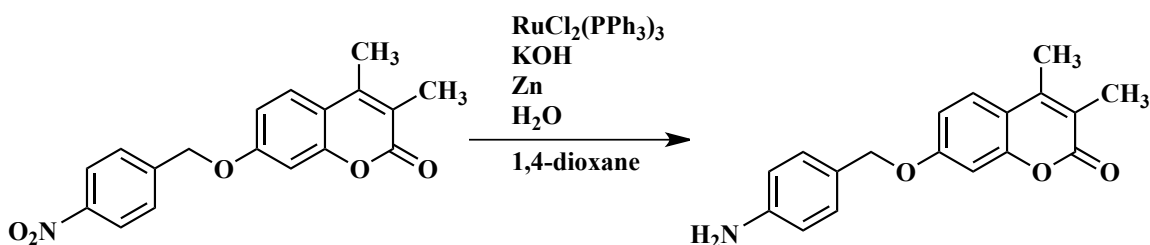
evaporated to yield a dark brown oil. Analysis by ^1H NMR in chloroform-*d* revealed the structure of the desired product.



First, 22 mg (0.13 mmol, 1 equiv.) of 7-hydroxy-4-methylcoumarin and a stir bar were added to a 25 mL round bottom flask. Next, 5 mL of 100% ethanol was added to the round bottom and stirring was initiated. Once the coumarin had fully dissolved, 17 mg (0.12 mmol, 1 equiv.) of potassium carbonate was added to the solution and the solution was stirred for 10 minutes before slow dropwise addition of 22 mg (12 mmol, 1 equiv.) of 4-aminobenzyl bromide dissolved in a minimal amount of 100% ethanol. After approximately 1/3 of the 4-aminobenzyl bromide had been added to the reaction mixture TLC (2:1 ethyl acetate: hexane) was taken, revealing no formation of a new spot. The reaction was next heated to $40\text{ }^\circ\text{C}$ and allowed to stir for 10 minutes. TLC of the reaction at this time revealed the emergence of a new spot. Slowly, the remainder of the 4-aminobenzyl bromide solution was added to the reaction mixture. After the final drop of 4-aminobenzyl bromide had been added the solution was allowed to stir for an additional 5 minutes before another TLC was taken. This TLC revealed the presence of some starting material still. Due to time constraints the solution was then acidified by addition of 2 M hydrochloric acid. This solution was then extracted three times using 10 mL portions of ethyl acetate. The aqueous phase was then made pH 6 by addition of 10% sodium hydroxide and extracted three more times with 10 mL portions of ethyl acetate. The organic phase was then dried over anhydrous sodium sulfate before being filtered

and evaporated. Analysis of the product by ^1H NMR using chloroform-*d* revealed collected product was not the desired product.

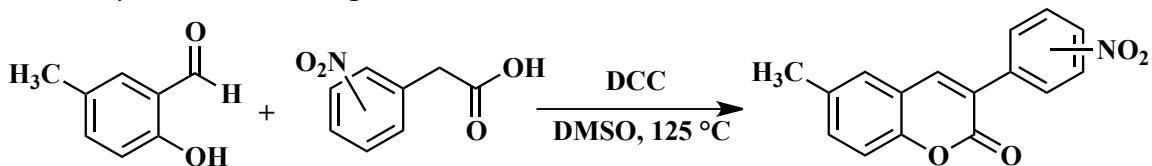
RuCl₂(PPh₃)₃ Mediated Reduction



To a 50 mL round-bottom flask, 53 mg (0.16 mmol, 1 equiv.) of 7-(4-nitrobenzyloxy)-3,4-dimethylcoumarin, 3.9 mg (2.5 mol %) $\text{RuCl}_2(\text{PPh}_3)_3$, 2.2 mg (25 mol %) potassium hydroxide, 35 mg (0.54 mmol, 3.4 equiv.) powdered zinc, 5 mL of water, and 5 mL of dioxane were added along with a stir bar. Next, 25 mL of acetone was added to the reaction mixture in order to aid in the dissolution of the coumarin. The solution was then refluxed for 48 hours, while stirring, before being analyzed by TLC using 1:1 ethyl acetate: hexane. TLC revealed two spots of similar R_f . The reaction at this point was hot filtered, then the pH was adjusted to 5 by addition of 1 M hydrochloric acid. Next, the solution was extracted with three 15 mL portions of ethyl acetate. The aqueous phase was kept and the solution was brought to pH 8 by addition of 5% sodium hydroxide. This phase was then extracted with a 15 mL portion of ethyl acetate, yielding a brown immulsion that was soluble in the aqueous phase. This solution was vacuum filtered and ^1H NMR was obtained using chloroform-*d* as solvent, which revealed the collected product was not the desired product.

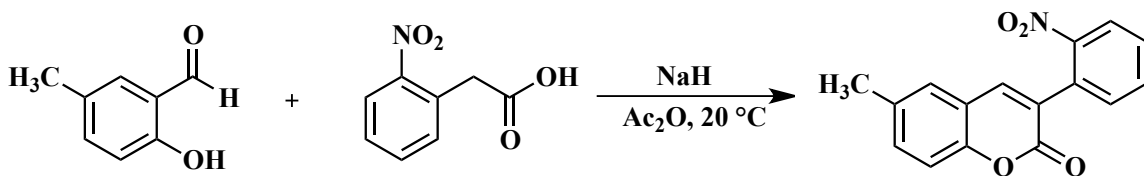
A1.2 Preparation of 3-nitrophenyl Substituted Coumarins

Perkin Style Reaction Using DCC



To a microwave reaction vial with stir bar 0.25 g (1.8 mmol, 1 equiv.) 2-hydroxy-5-methylbenzaldehyde, 0.6 g (2.9 mmol, 1.6 equiv.) N,N'-dicyclohexylcarbodiimide, and 0.42 g (2.3 mmol, 1.3 equiv.) of the appropriately substituted nitrophenylacetic acid were added, followed by 7 mL of dimethyl sulfoxide. The reaction was then run at 125 °C for 7 minutes before being stopped and poured over concentrated acetic acid on ice and being allowed to sit for two hours. The reaction product was then extracted with three 25 mL portions of diethyl ether. The organic portions were then washed with 50 mL of 5% sodium bicarbonate and, lastly, with 20 mL of brine solution. The solvent was evaporated and a ^1H NMR in chloroform-*d* was obtained, revealing a convolution of peaks. Because it was not clear if the product was present flash chromatography in 1:1 ethyl acetate:hexane was performed. The separated components were evaporated and ^1H NMR was taken again, revealing that the desired product had not been formed.

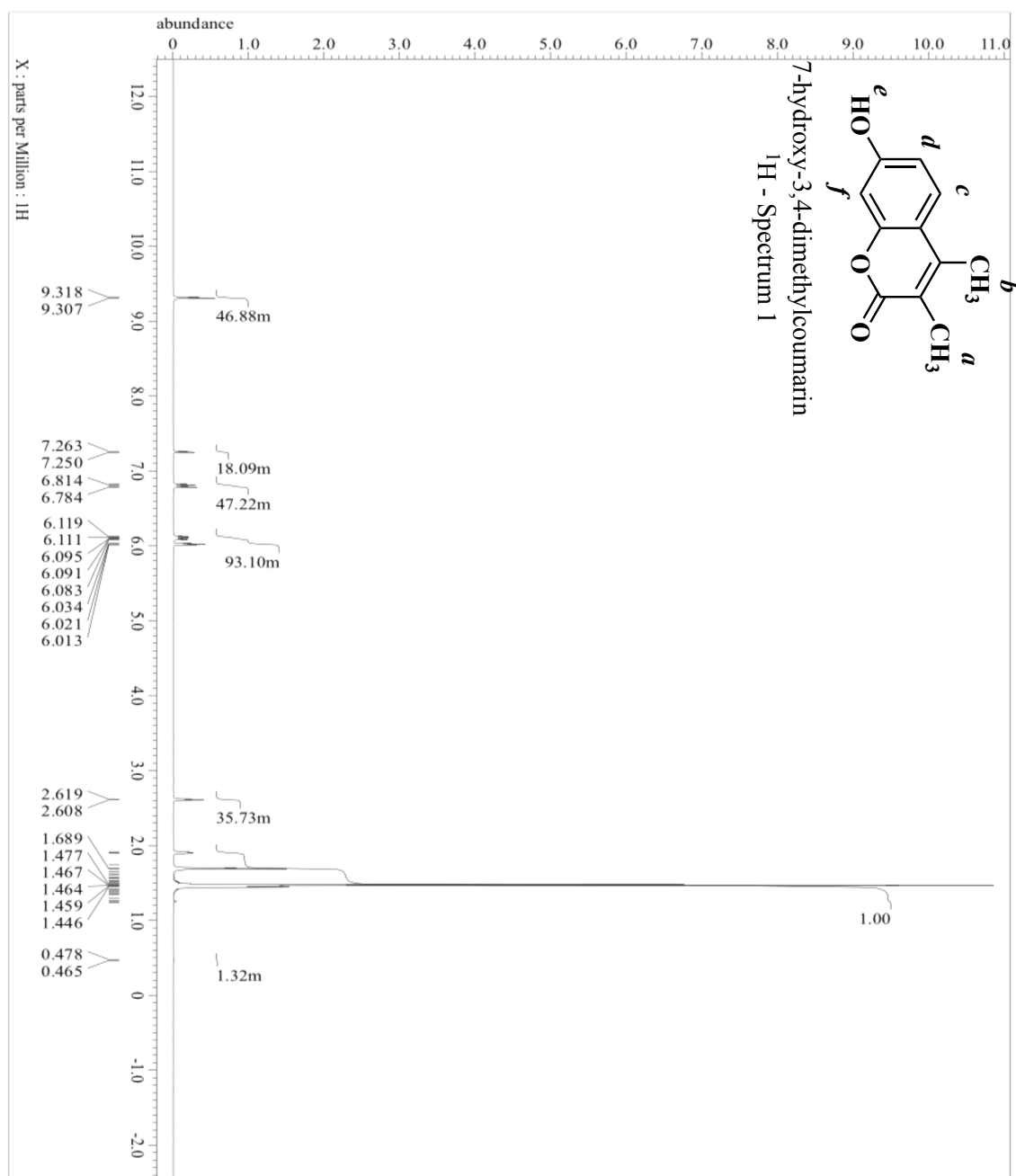
Modified Perkin Reaction

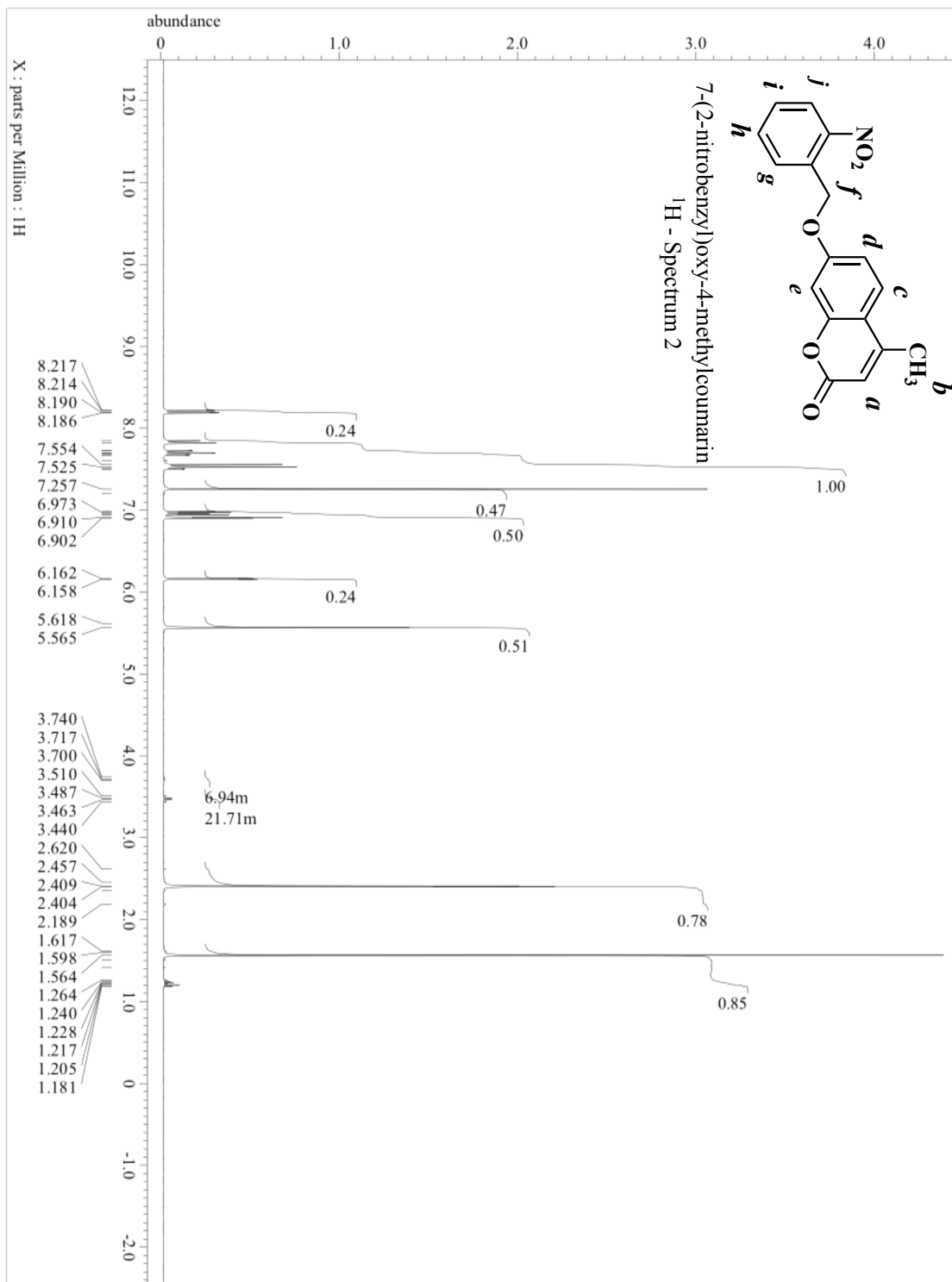


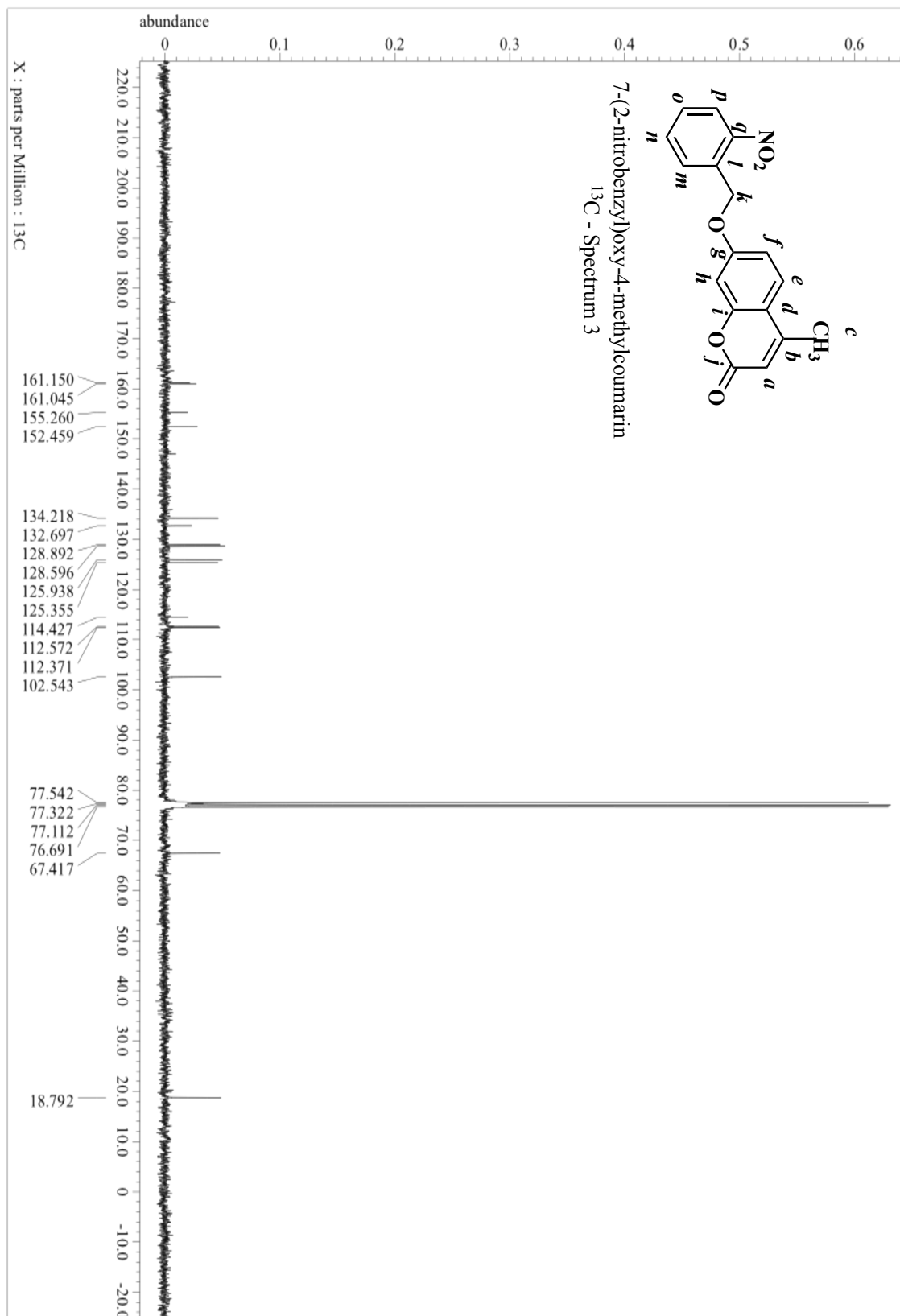
To a 10 mL round-bottom flask 0.25 g (1.8 mmol, 1 equiv.) 2-hydroxy-5-methylbenzaldehyde, 0.33 g (1.8 mmol, 1 equiv.) 2-nitrophenylacetic acid (4-nitrophenylacetic acid was also attempted), and stir bar were added. Next, the flask was

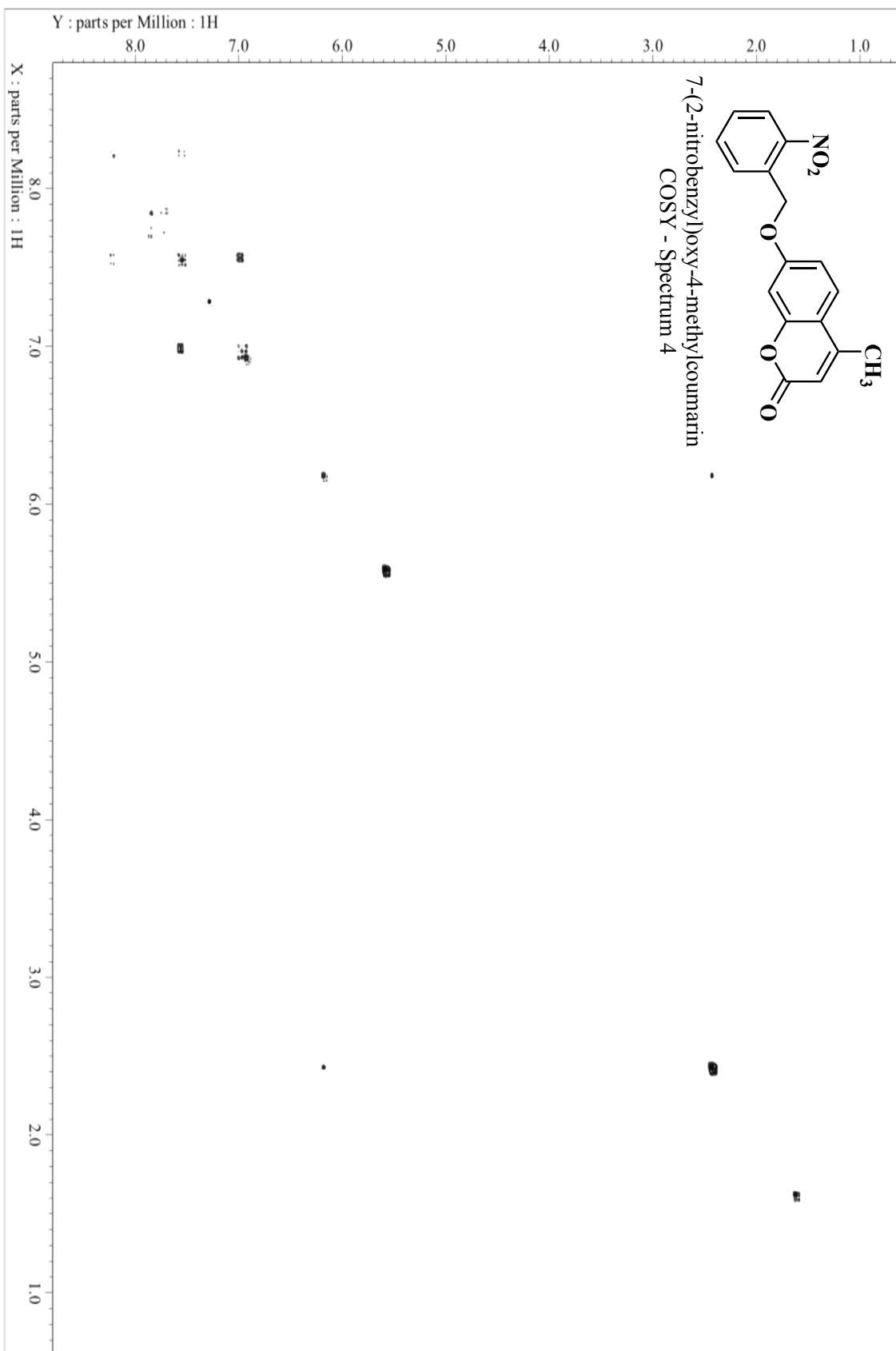
capped, evacuated, and purged with argon before the addition of 2.0 mL (21 mmol, 21 equiv.) of acetic anhydride. The flask was again capped, evacuated, and purged with argon. Stirring was initiated. Next, 0.16 g (4.0 mmol, 4 equiv.) sodium hydride (60% dispersion in mineral oil) was then added to the solution in small portions before the reaction was capped and allowed to stir for three hours. The reaction was monitored by thin layer chromatography using 1:9 ethyl acetate: hexane as solvent. After this time the reaction was gravity filtered to remove solid. The solid was washed with ethyl acetate and the filtrate was then extracted with three 20 mL portions of 5% sodium bicarbonate. The organic phase was then dried over anhydrous magnesium sulfate before being gravity filtered into a 100 mL round-bottom flask and evaporated. ^1H NMR of the collected solid in chloroform-*d* revealed that the collected product was not the desired product.

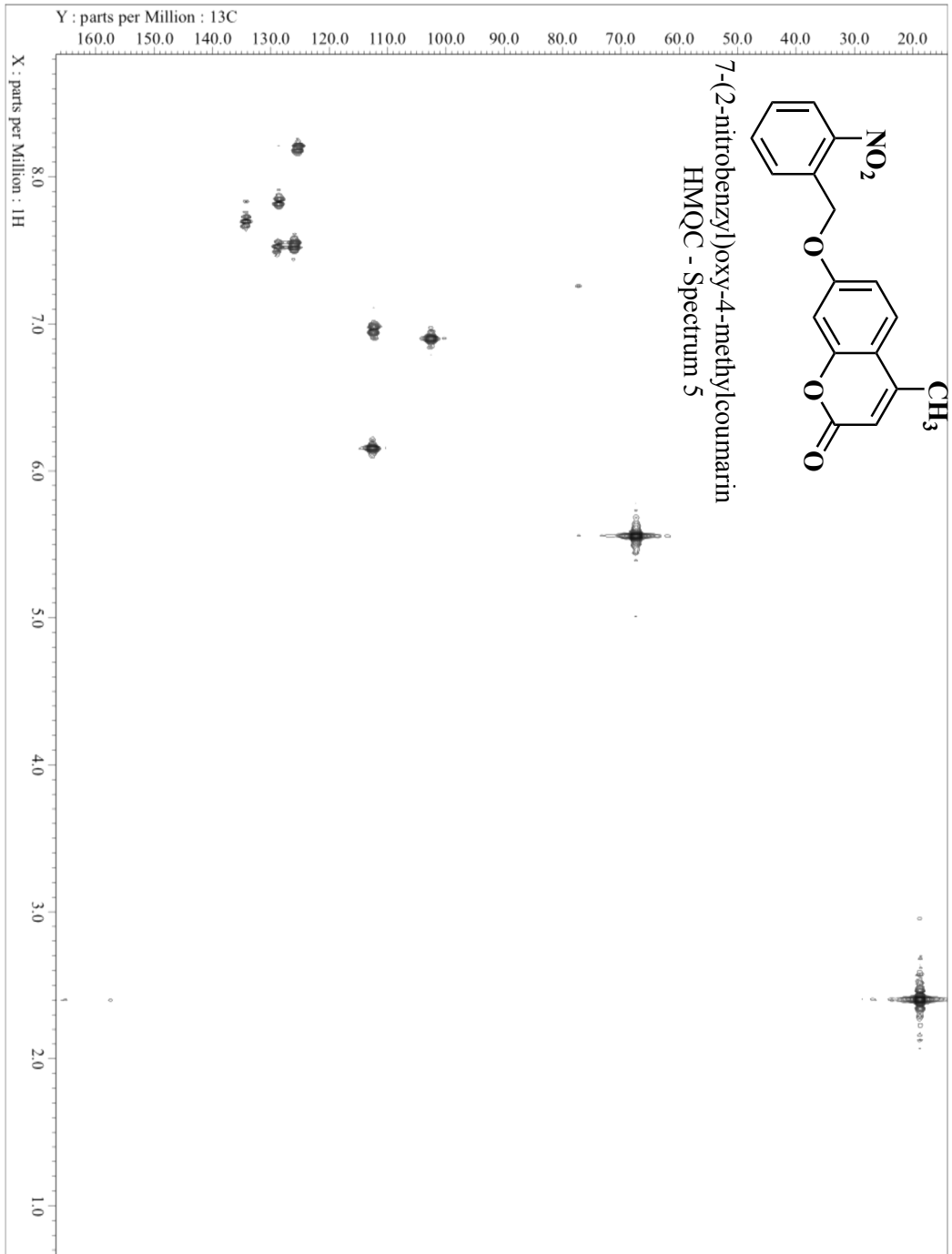
Appendix B. Synthesis Characterization Spectra

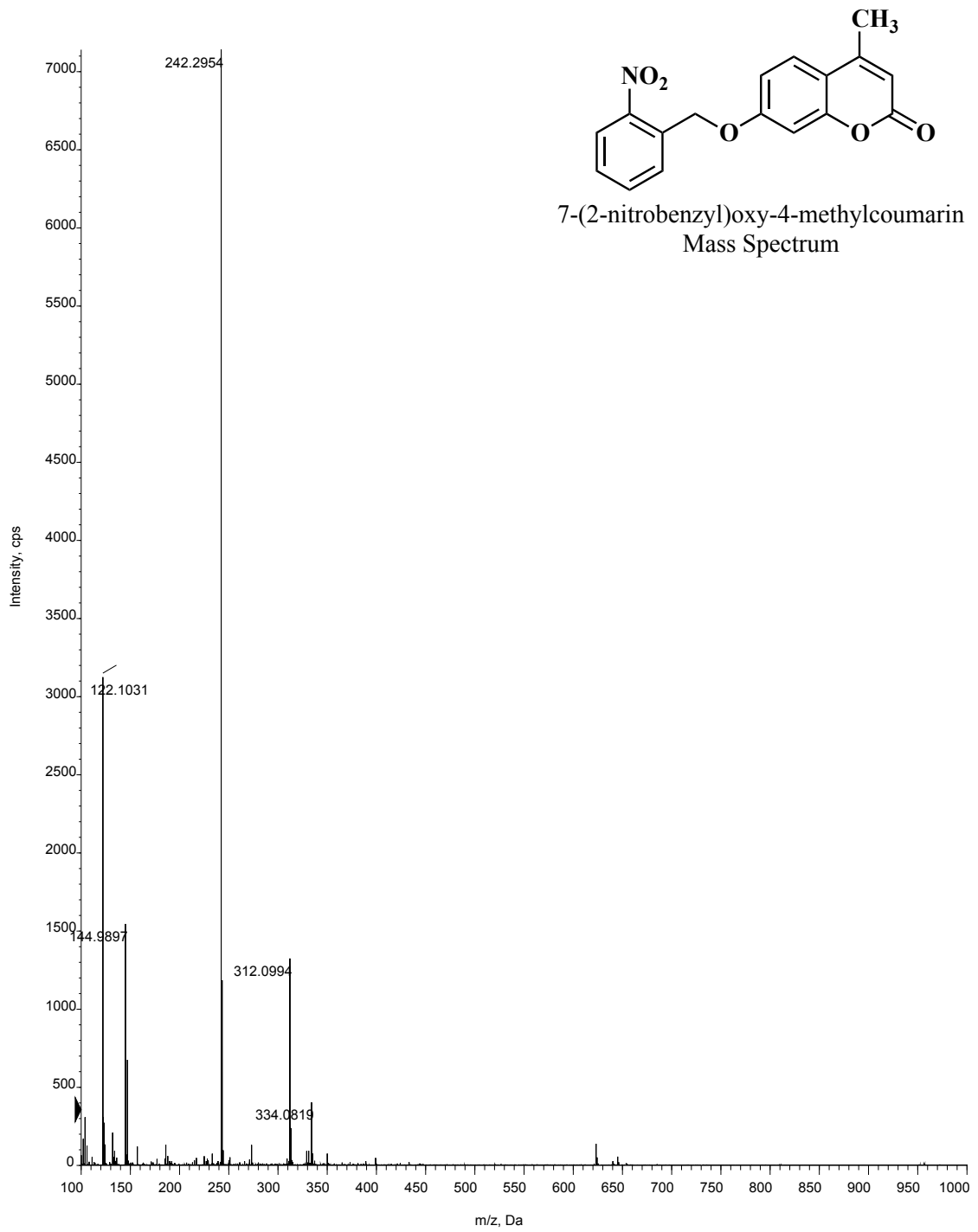


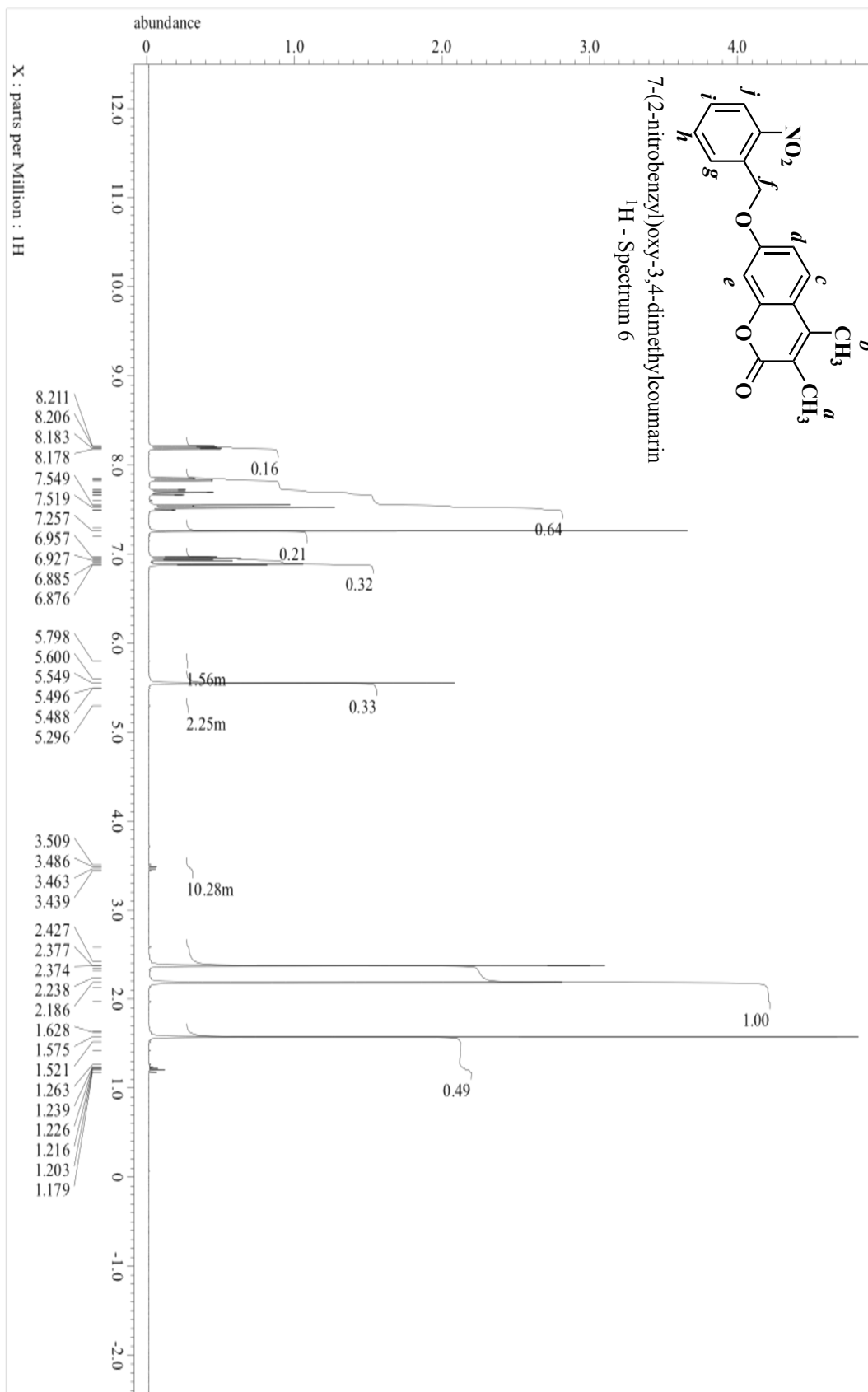


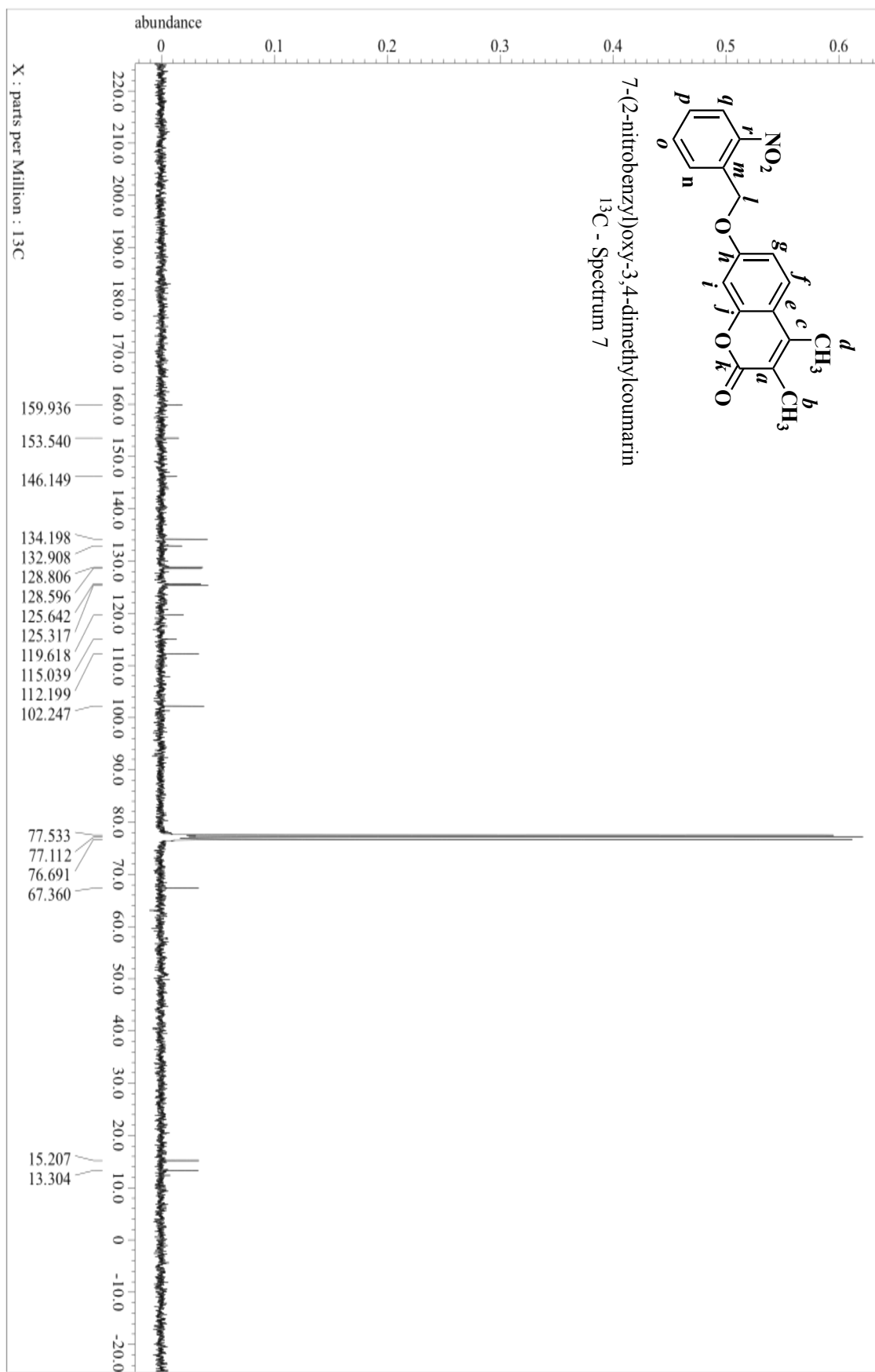


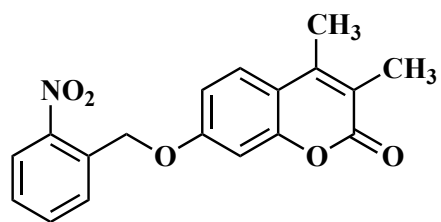




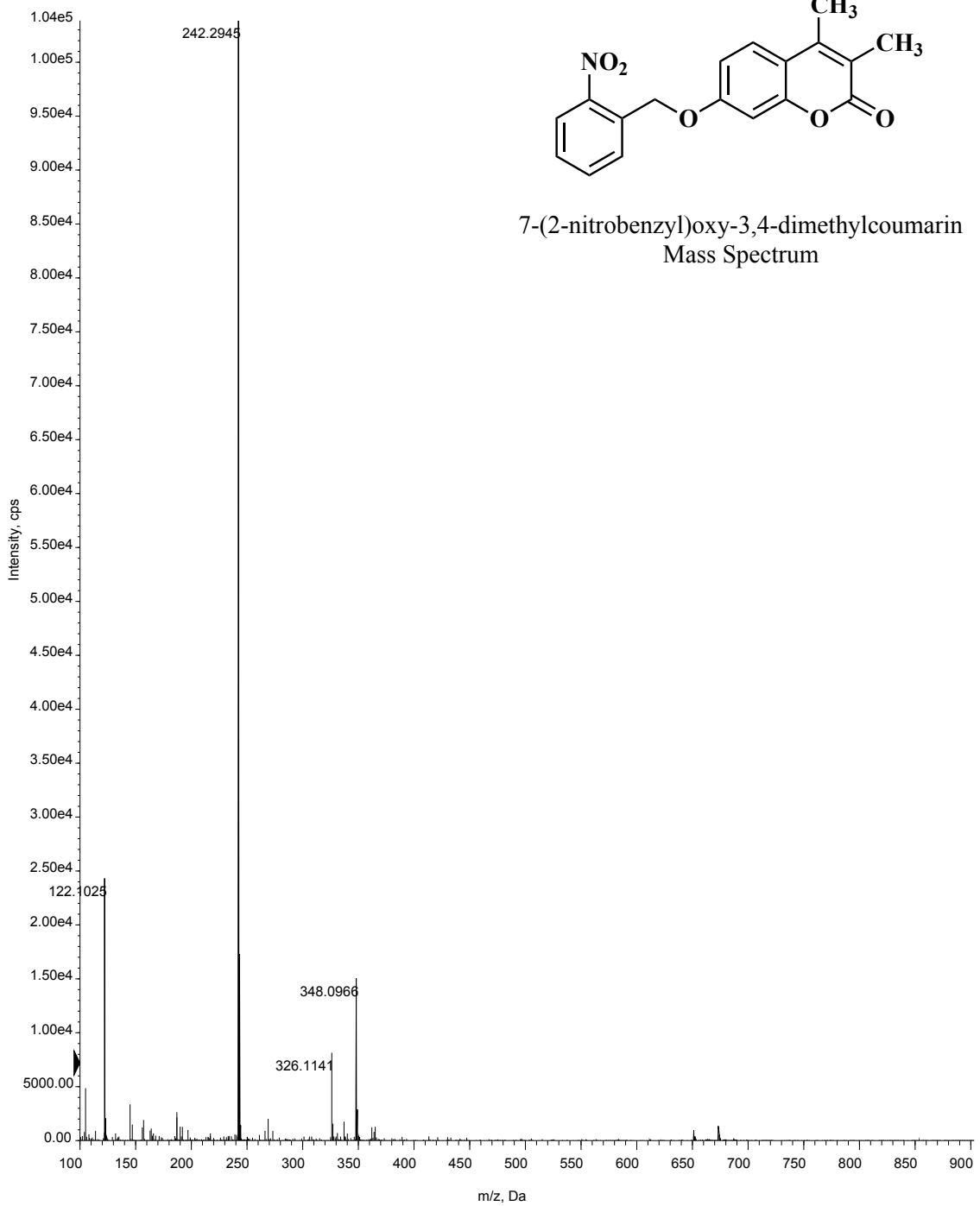


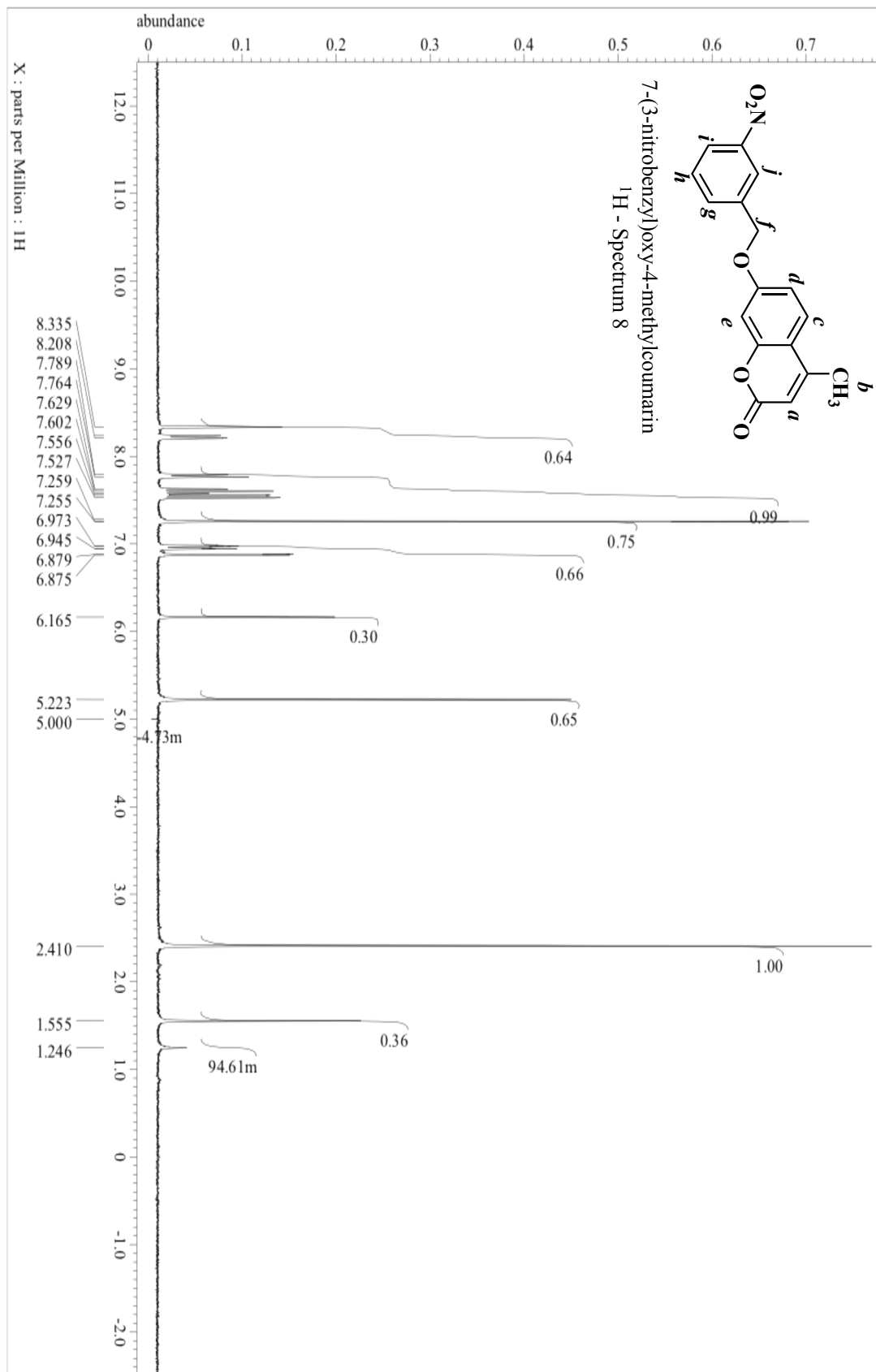


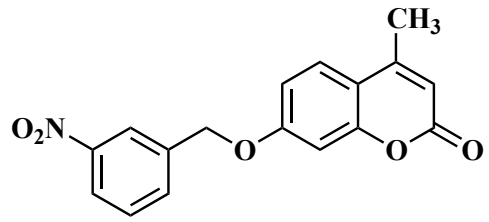




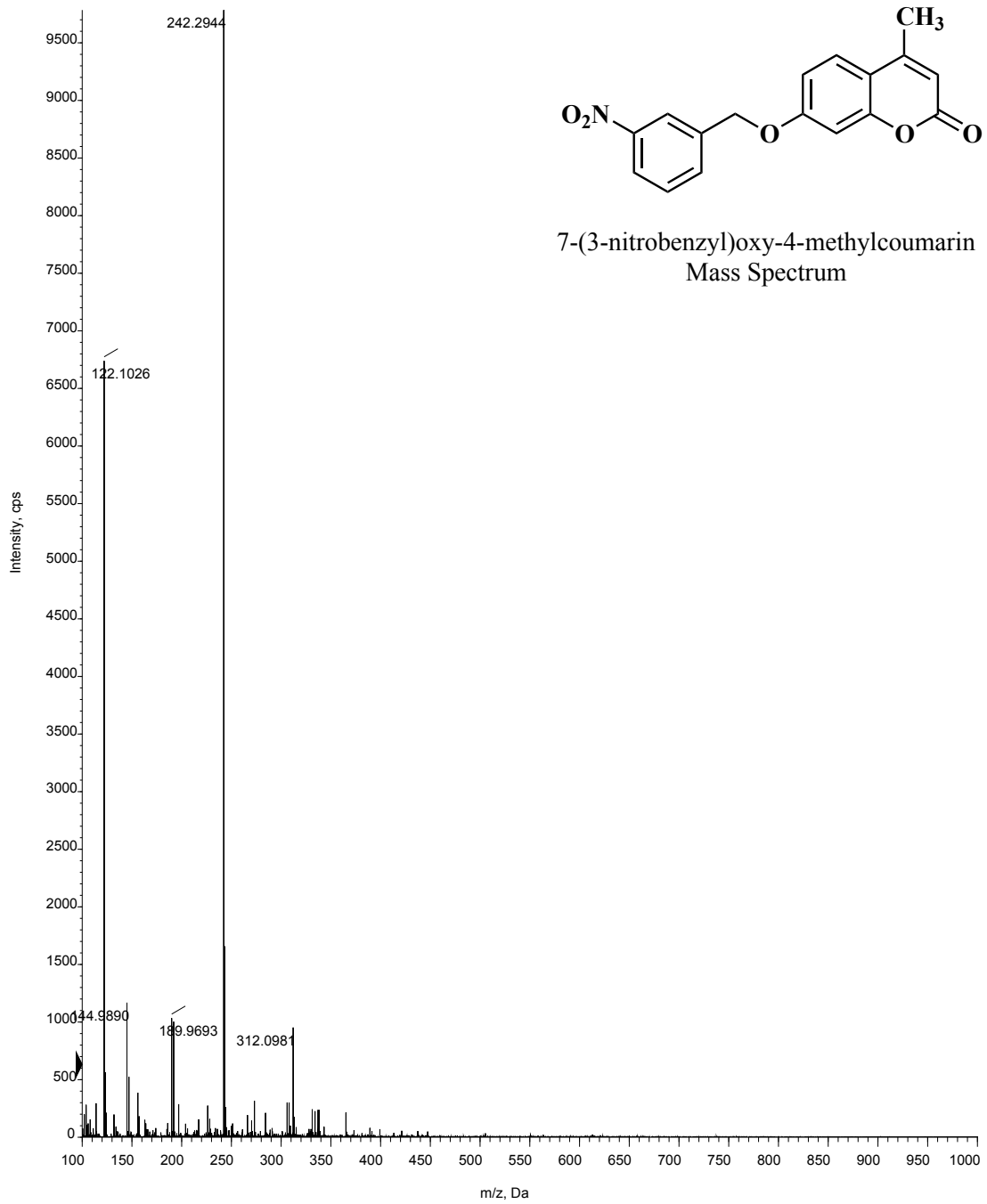
7-(2-nitrobenzyl)oxy-3,4-dimethylcoumarin
Mass Spectrum

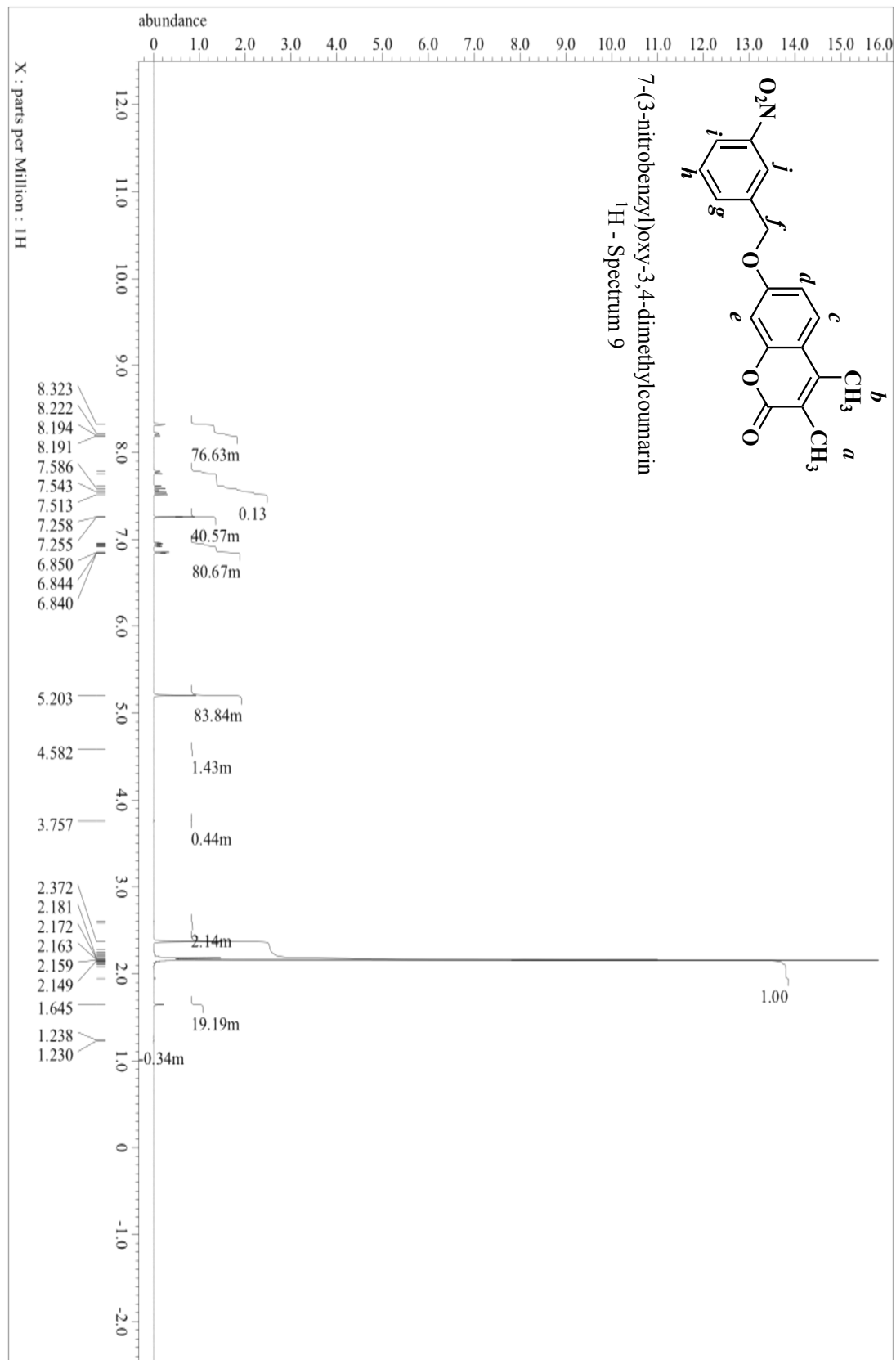


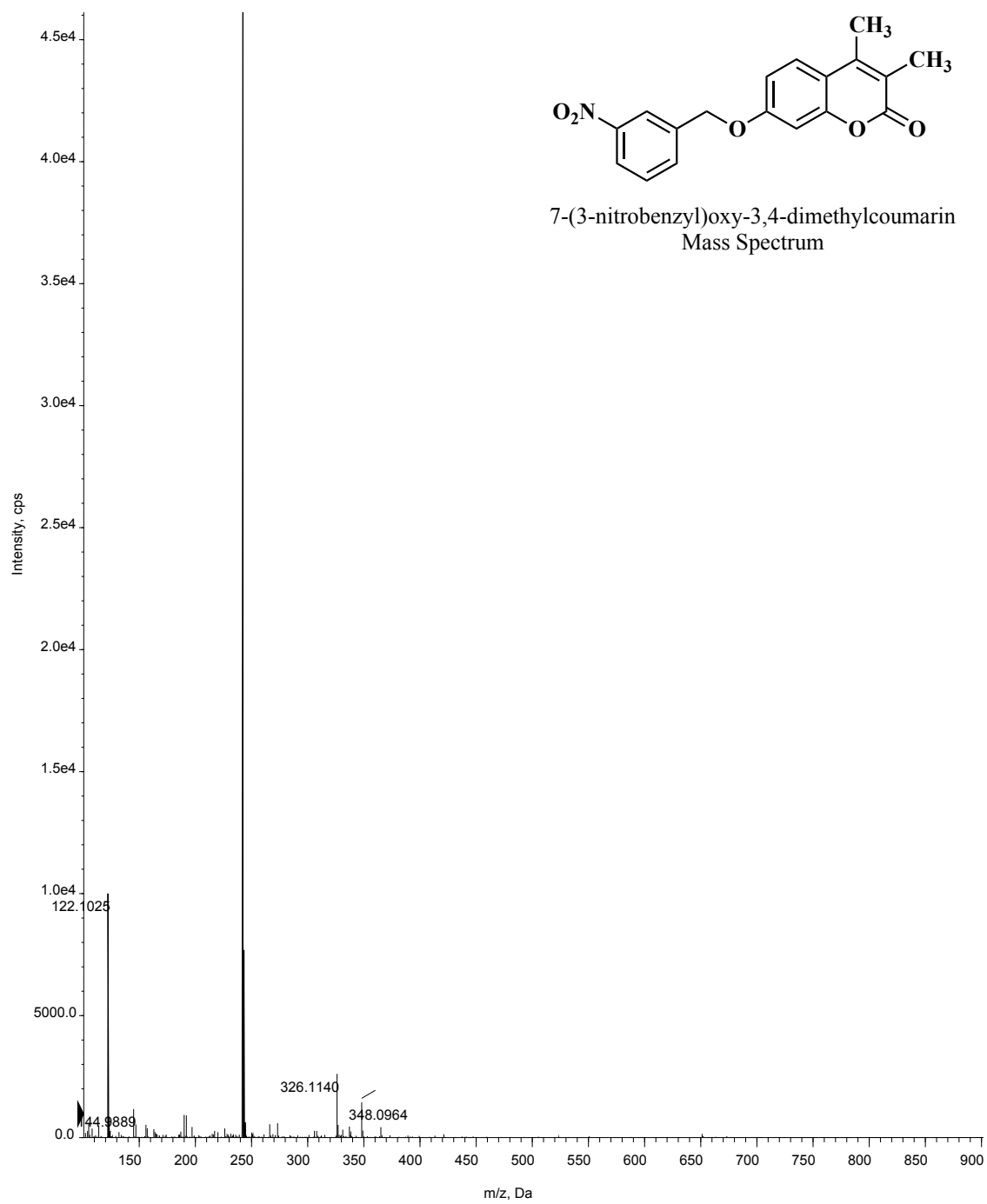


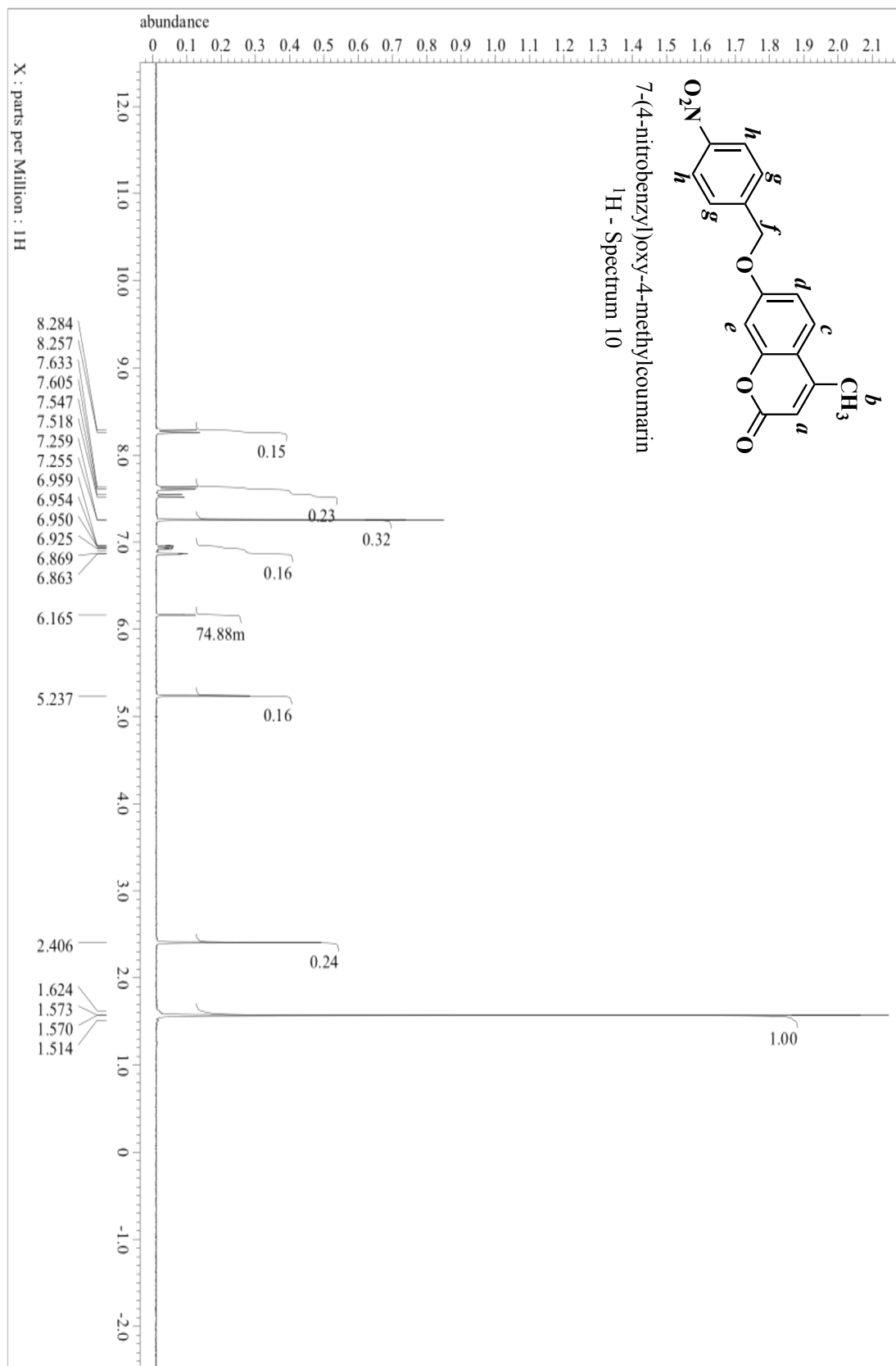


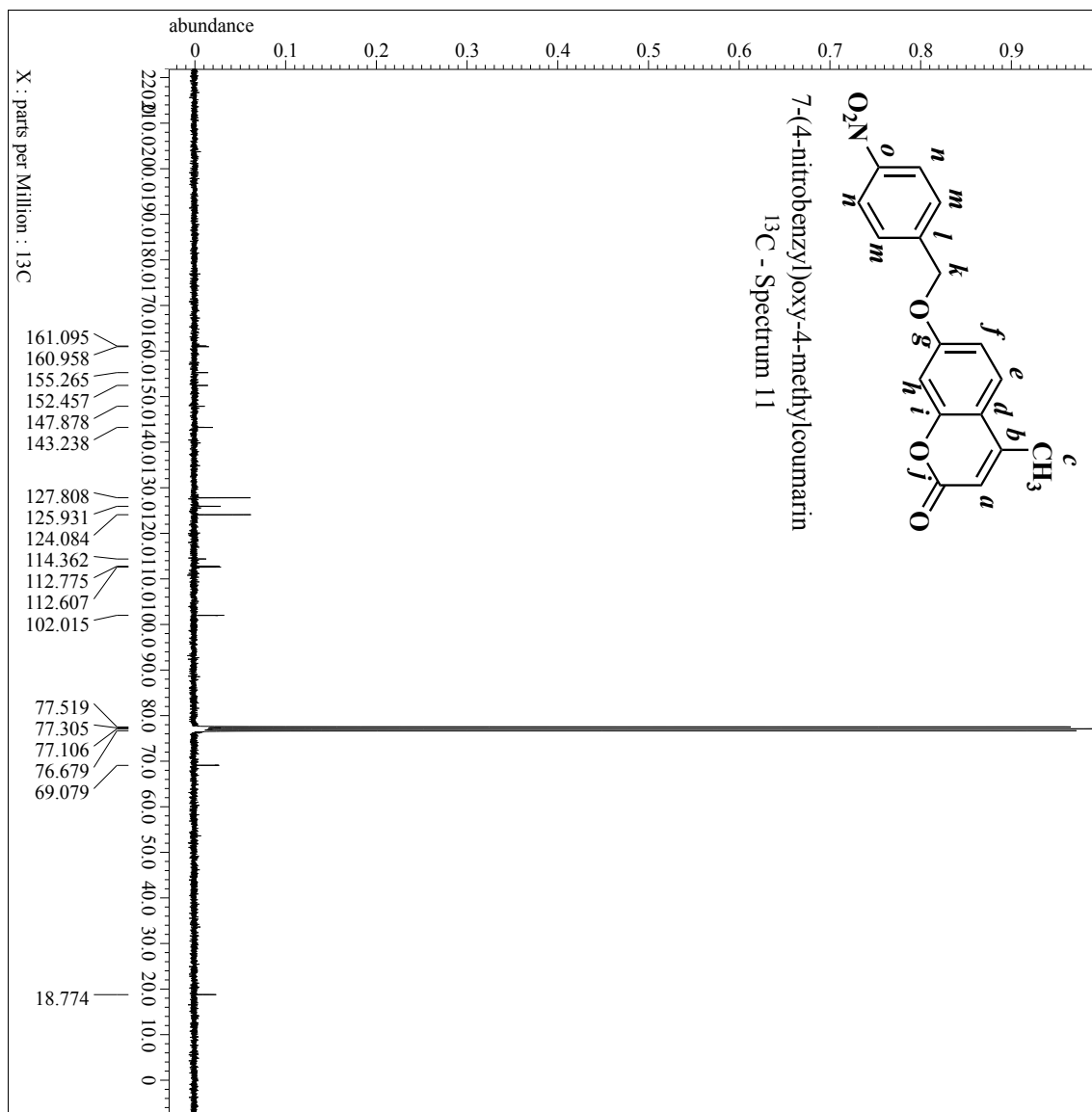
7-(3-nitrobenzyl)oxy-4-methylcoumarin
Mass Spectrum

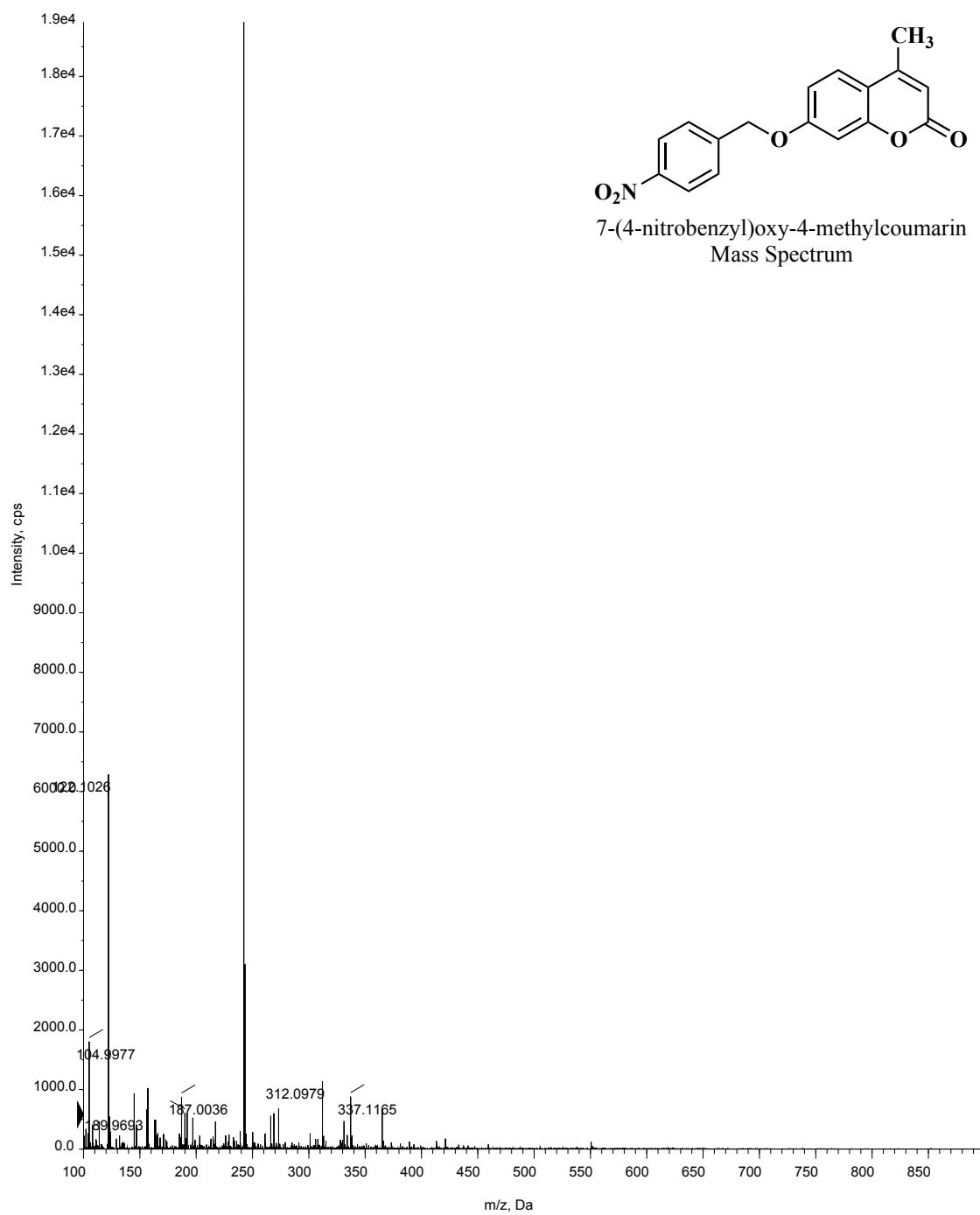


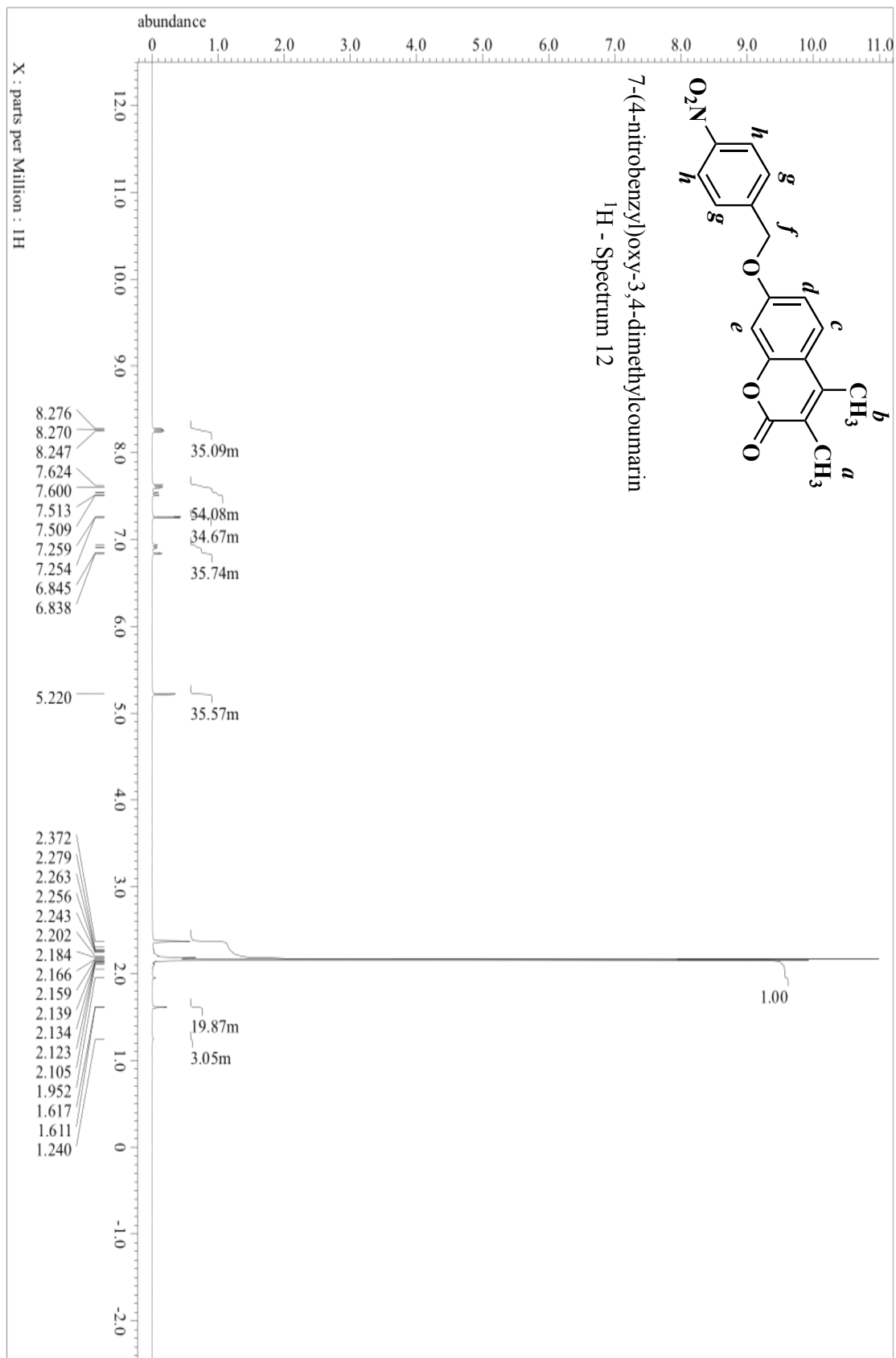


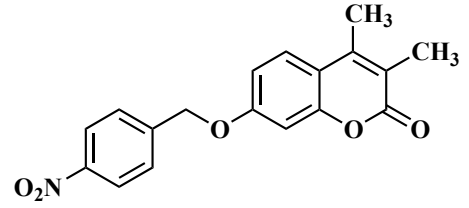




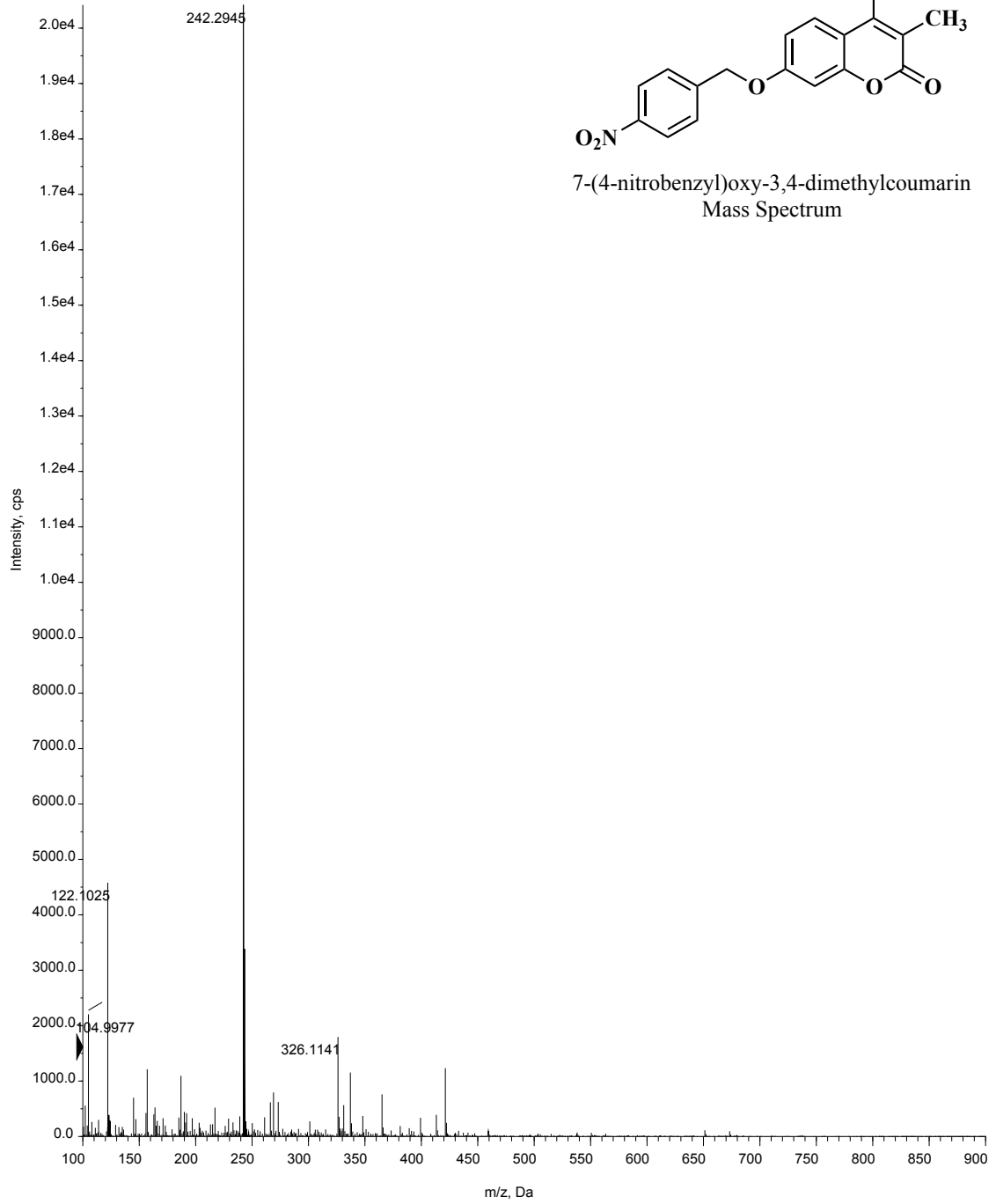


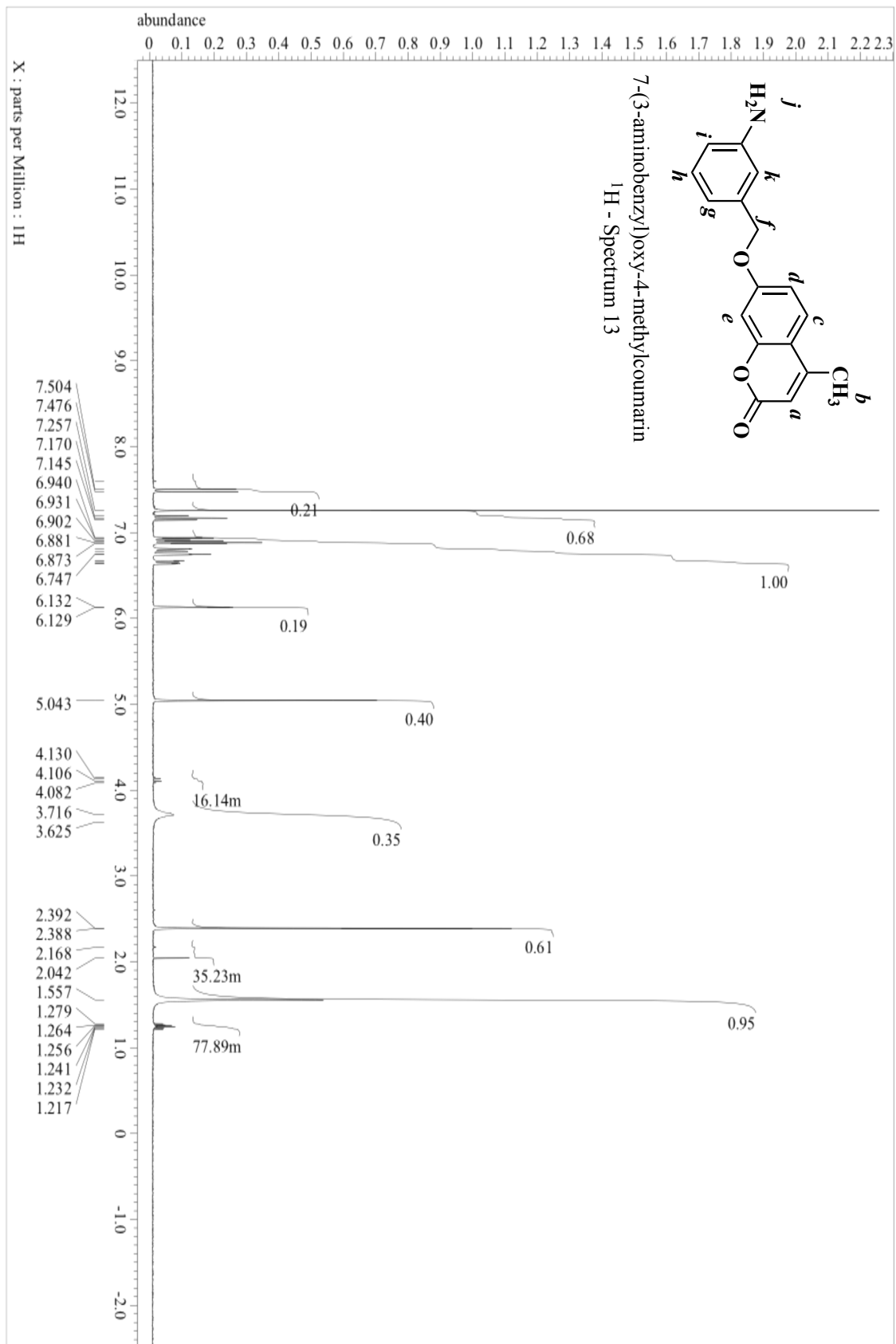


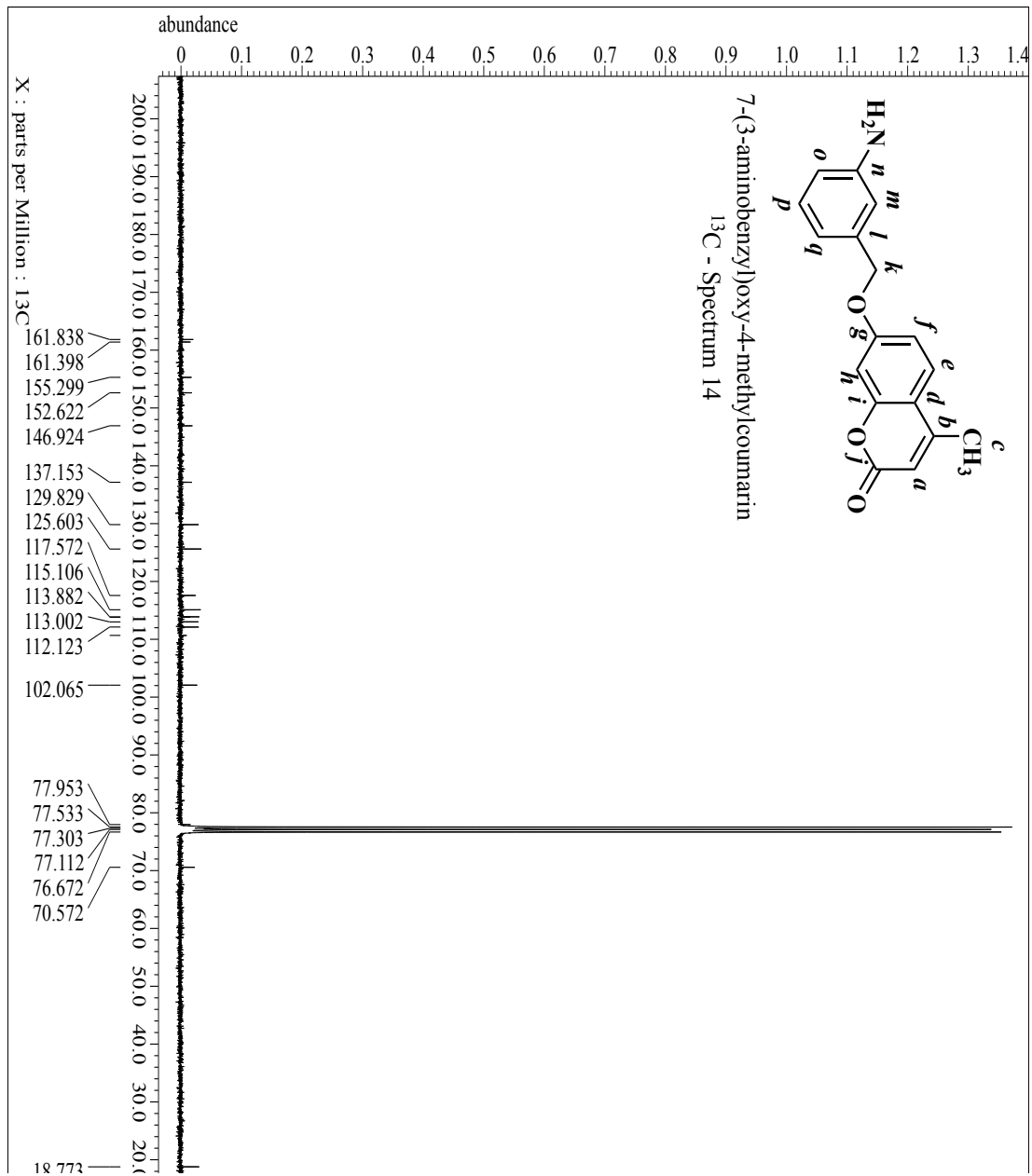


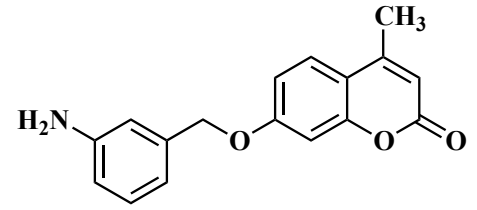


7-(4-nitrobenzyl)oxy-3,4-dimethylcoumarin
Mass Spectrum









7-(3-aminobenzyl)oxy-4-methylcoumarin
Mass Spectrum

